

UNIVERSITY OF WASHINGTON

DEPARTMENT OF  
OCEANOGRAPHY

Royse 1964  
conclusions on  
Pg. 40

Technical Report No. 111

SEDIMENTS OF WILLAPA SUBMARINE CANYON

by

Chester F. Royse, Jr.

U.S. Atomic Energy Commission

Contract AT(45-1)-1725

and

Office of Naval Research

Contract Nonr-477(10)

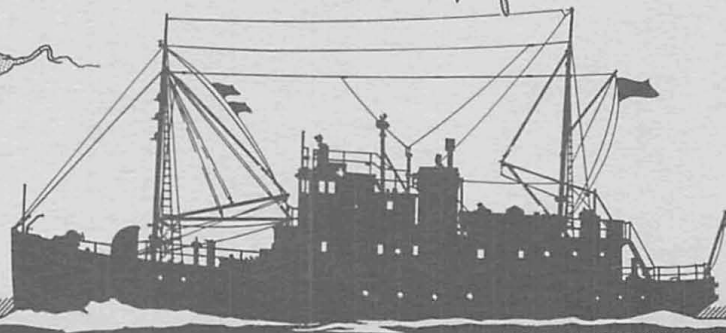
Project NR 083 012

Contract Nonr-477(37)

Project RR 004-03-01

Reference M64-60

September 1964



SEATTLE, WASHINGTON 98105

UNIVERSITY OF WASHINGTON  
DEPARTMENT OF OCEANOGRAPHY  
Seattle, Washington 98105

Technical Report No. 111

SEDIMENTS OF WILLAPA SUBMARINE CANYON

by

Chester F. Royse, Jr.

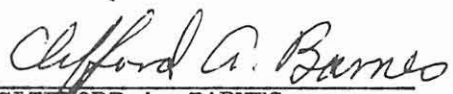
U.S. Atomic Energy Commission  
Contract AT(45-1)-1725

and

Office of Naval Research  
Contract Nonr-477(10)  
Project NR 083 012

Contract Nonr-477(37)  
Project RR 004-03-01

Reference M64-60  
September 1964

  
CLIFFORD A. BARNES  
ACTING CHAIRMAN AND  
PRINCIPAL INVESTIGATOR

Reproduction in whole or in part is permitted  
for any purpose of the United States Government

## SEDIMENTS OF WILLAPA SUBMARINE CANYON

## ABSTRACT

A study of Willapa Submarine Canyon, located off the Washington coast, was undertaken in an attempt to define the type, distribution, and rate of deposition of sediment within the canyon.

Well sorted sands are common on the continental shelf near the canyon head and green pelagic muds predominate within the canyon. The muds are thinly bedded and cores from the thalweg contain sand layers. Organic- and carbonate-carbon contents of sediments range between 0.2-2.9 and 0.05-1.5 per cent respectively. The clay-sized fraction of the average sediment consists of approximately 20 per cent Fe-chlorite, 30 per cent kaolinite, and 50 per cent illite with minor amounts of montmorillonoids and mixed-layer clays.

Analyses of the heavy-mineral and clay-mineral suites show that the Columbia River is the most probable source of sand and mud in the canyon. The occurrence of graded sand layers containing shallow water foraminifera and heavy mineral suites similar to those of shelf sands indicate turbidity-current transport of shelf sediment along the canyon axis.

The maximum rate of sedimentation on the upper slope is about  $50 \text{ mg cm}^{-2}\text{yr}^{-1}$  (41 centimeters per thousand years), but the total thickness of Holocene sediment in most of the canyon is only a few meters. Turbidity flows, originating on the upper slope and shelf, deposit the major portion of their sediment load west of the slope break in Cascadia Basin.

Rock dredged from the canyon walls contains fossils which suggest Willapa Canyon has formed since early-Pliocene time.

## ACKNOWLEDGMENTS

The author is indebted to the following members of the Department of Oceanography for their assistance in the preparation of this report: Drs. Joe S. Creager, M. Grant Gross, Lawrence K. Coachman, Dean A. McManus, Betty J. Enbysk, and Mr. Donald Doyle and his staff of illustrators. Assistance in collection and analysis of samples is gratefully acknowledged from: Mrs. Marsha Wallin, Mr. Larry Hansen, Mr. James Baker, Mr. Robert Andrews, Mr. George Hoskins, Mr. Robert Cooney, Lt. Ray Moses (USC&GS), and the officers and crew of the M.V. Brown Bear.

This work was supported by the United States Atomic Energy Commission, Contract AT(45-1)-1725 and the Office of Naval Research, Contract Nonr-477(10), Project 083-012, and Contract Nonr-477(37), Project RR 004-03-01.

## TABLE OF CONTENTS

INTRODUCTION .....	1
Scope and Objectives .....	1
Description and Bathymetry .....	1
Previous Work .....	1
FIELD WORK .....	4
ANALYTICAL METHODS AND PRESENTATION OF DATA .....	4
Texture and Composition of Sediments .....	4
Size Components .....	5
Sorting .....	5
Mean and Median Grain-Size .....	5
Skewness .....	5
Carbon and Nitrogen Content .....	12
Water Content .....	12
Heavy-Mineral Suites .....	15
Light-Mineral Suites .....	16
Clay Minerals .....	18
Foraminifera .....	18
Wall Rock .....	28
Depositional Rates .....	28
DISCUSSION AND INTERPRETATION .....	29
Description of Sediments .....	29
Source of Sediments .....	30
Lithogenous Material .....	30
Organic Matter .....	33

## Table of Contents (continued)

Calcium Carbonate .....	34
Pre-Holocene Sediments .....	35
Sediment Transport .....	35
Grain-Size Distributions .....	35
Displaced Fauna .....	36
Turbidity Currents .....	37
Depositional Rates .....	38
Willapa Ash .....	38
CONCLUSIONS .....	40
REFERENCES .....	41
APPENDIX I .....	45
APPENDIX II.....	58
APPENDIX III.....	62

## LIST OF FIGURES

1. Index chart .....	2
2. Bathymetry and sample locations .....	3
3. Sand, silt, clay contents of samples .....	10
4. Sorting as a function of mean grain-size .....	11
5. Carbonate-carbon content as a function of mean grain-size .....	13
6. Organic-carbon content as a function of mean grain-size .....	14
7. X-ray diffractograms of samples from core 326-52 .....	32
8-18. Sediment parameters versus depth in cores .....	46-57
19. Sediment parameters of surface samples .....	57
20. X-ray diffractograms showing results of glycol, acid, and heat treatments .....	61

## LIST OF TABLES

1. Sample locations and size data .....	6
2. Water content of samples from core 326-36 .....	15
3. Heavy-mineral percentages of selected samples from the canyon rim and lower canyon .....	16
4. Heavy-mineral compositions of selected samples from the canyon rim and lower canyon.....	17
5. Intensity ratios of major X-ray diffraction peaks of surface samples and their estimated illite:Fe- chlorite:kaolinite ratios.....	19
6. Intensity ratios of major X-ray diffraction peaks for the clay-size sediment in untreated samples from four cores .....	20
7. Foraminifera in surface samples .....	22-26
8. Foraminifera in selected cores .....	27
9. Estimated depositional rates of sediment components in core 326-36 .....	29

## INTRODUCTION

### Scope and Objectives

The general scope of this investigation of Willapa Submarine Canyon is that of a reconnaissance with the following objectives: 1) to define the general character and distribution of sediment; 2) to determine the nature and rate of sediment deposition; and 3) to determine the mode and extent of bottom transport within Willapa Canyon.

### Description and Bathymetry

Willapa Canyon heads about 30 kilometers off the Washington coast in the vicinity of  $46^{\circ}30'$  N latitude and extends westward about 110 kilometers where it swings southward and enters Cascadia Basin (Figure 1).

Willapa Canyon, with its tributary, Guide Canyon, is only one of the canyons in the continental terrace off Washington and is comparable in size to Astoria Canyon to the south and Grays Canyon to the north (Figure 2). There are numerous smaller, unnamed canyons in the area. The total relief in longitudinal profile (from canyon head to mouth) is about 1200 fathoms (2200 meters). The maximum average slope of the canyon walls is 30-40 degrees and their maximum relief, in deeply incised areas, is about 600 fathoms (1100 meters).

The canyon can be divided into upper and lower regions (Figure 1) at the 1000-fathom isobath. The upper canyon area includes Willapa and Guide Canyons and is characterized by great relief and steep canyon walls. Near the 1000-fathom isobath, Guide Canyon joins Willapa Canyon and their combined axis passes through a narrow gorge into the lower canyon area.

The lower canyon has less relief than the upper canyon, its walls slope more gently and its floor is broader. Tributary channels appear to enter the major axis from both the north and south. Near the slope break (approximately the 1300-fathom isobath) the canyon axis breaches a series of northwest trending ridges and enters Cascadia Basin.

### Previous Work

Since 1930 when the United States Coast and Geodetic Survey began charting the continental terrace, data on submarine canyons have accumulated rapidly. Early work was primarily devoted to locating, describing and comparing the morphology of canyons (Shepard and Beard, 1938; Shepard and Emery, 1941) and few studies were made of the sediments in the canyons. Among these were the study of the geology and paleontology of Georges Bank Canyons (Stetson, 1936) and a comparative study of the sediments of canyons off the California coast (Cohee, 1938). Recent studies by Gorsline and Emery (1959) and Emery and Hulsemann (1963)

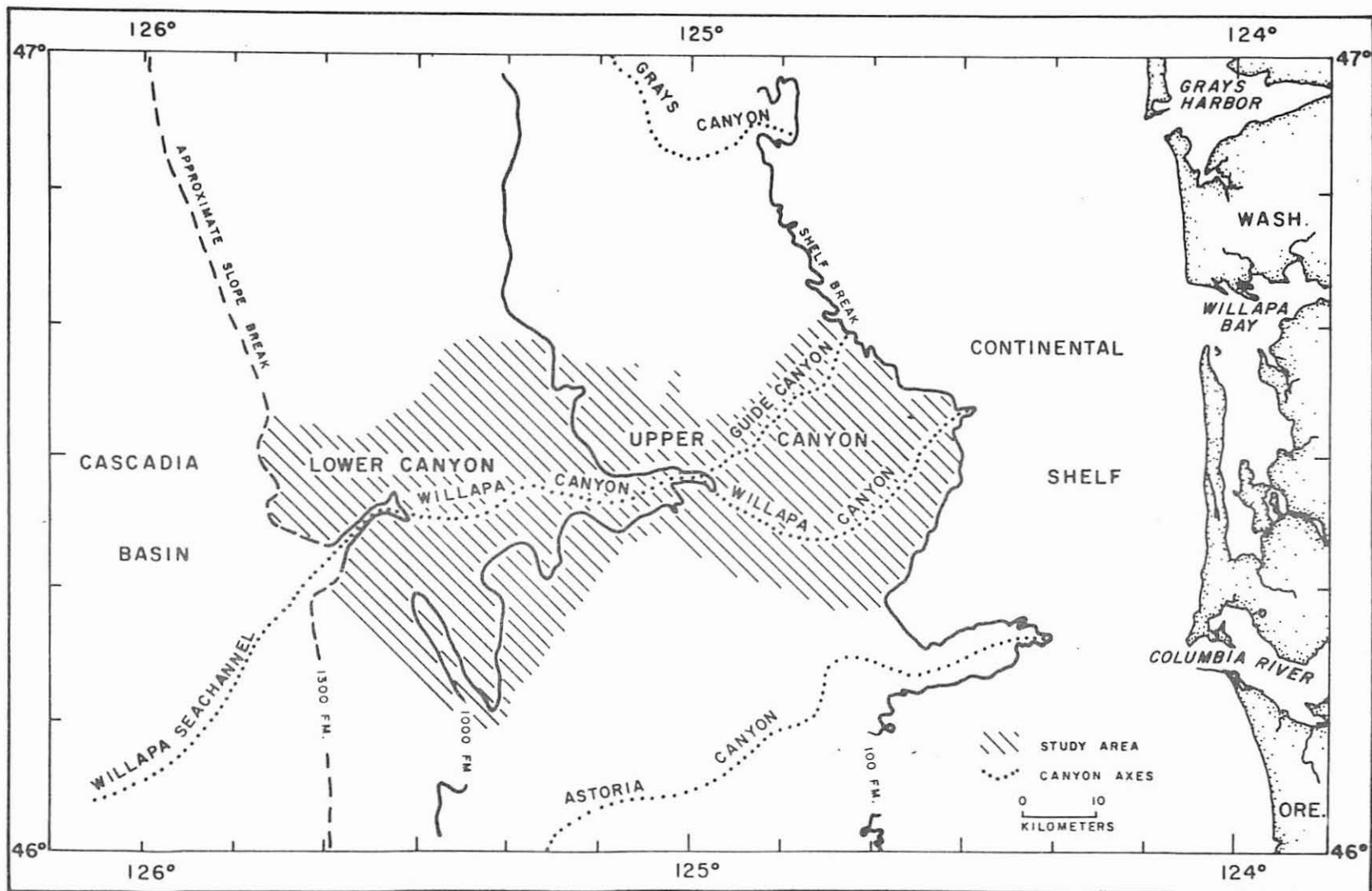


Fig. 1. Index chart.



have related sediment textures and distribution to transport along canyon axes. Classification, description, and comparative relationships of submarine canyons have been given by Emery (1960) and Shepard (1963a, 1963b).

Willapa Canyon has not been studied before, but the general nature of sediment distribution on the adjacent shelf, the Columbia River Delta, and Cascadia Basin are known (Shepard, 1939, p. 224; B. J. Enbysk and D. A. McManus, personal communication).

#### FIELD WORK

Sediment samples were collected in June, 1963 from the M.V. Brown Bear (cruise 326). Sample locations (including samples taken on Brown Bear cruises 291 and 312) are shown in Figure 2.

A 24-liter Van Veen sampler (Van Veen, 1936) with a maximum penetrating depth of 23 centimeters was intended for use near the canyon head, but one sample (station 326-37) was obtained at a depth of 572 fathoms (1100 meters). Samples from deeper water were taken with a 7.35-centimeter diameter, 3.5-meter long Kullenberg-type piston corer (Kullenberg, 1947). A 3.87-centimeter diameter gravity corer (trigger corer), 30 centimeters long, was used to initiate the one-meter piston corer free fall. Coring was attempted at all stations, but mechanical failures and high seas resulted in no recovery at several stations. A steel-pipe dredge, 45 centimeters in diameter and about 1.5 meters long, was used at three localities to obtain samples of the canyon walls. The cores were sealed in the liners, labeled, and secured in an upright position aboard ship. Van Veen samples, trigger cores, and dredge hauls were frozen to retard decomposition of organic matter.

Station positions were located by Loran-A, which has an approximate accuracy of one per cent of the distance between the ship and the transmitters (Von Arx, 1962). This gave an accuracy of  $\pm 0.5$  nautical miles ( $\pm 930$  meters) within the study area. Sampling depths and the bathymetry between stations were determined with an EDO AN/UNQ 2-B echo sounder and recorder. Loran positions were corrected for wind and current drift and adjusted to the bathymetry of the chart in Figure 2. A continuous bathymetry track was not run.

#### ANALYTICAL METHODS AND PRESENTATION OF DATA

##### Texture and Composition of Sediments

Detailed studies of samples from Brown Bear cruise 326, supplemented by size and foraminiferal data from Brown Bear cruises 291 and 312, form the basis for this discussion. Samples are designated by cruise and station number and by sampler type or sample depth in cores. Details of sampling techniques are given in Appendix II.

Size analyses (Appendix II) were made for each sample and statistical parameters of size distributions computed (Creager, McManus, and Collias, 1962). The statistical parameters of Folk and Ward (1957) and the second skewness and kurtosis of Inman (1952) could seldom be calculated because most sediment size distributions were open ended. No Inman values were calculated for samples in which the next to last accumulated percentages of size classes was less than 84. Inman mean, median, deviation, and skewness were obtained for most samples (Table 1) and are used in this study.

Size Components:--The sand, silt, and clay relationships shown on the three-point diagram of Figure 3 (Shepard, 1954) indicate that the sediments group into two end-members, one consisting of high percentages of sand and a second of nearly equal parts of silt and clay with less than 5 per cent sand. A third sediment type is composed of mixtures of these end-members. The end-members are shelf sand (shelf sediment containing greater than 75 per cent, dry weight, sand-sized material) and slope mud (sediment consisting predominantly of clay-silt sized particles); mixed sediments come from the shelf and the slope. The nearly equal amounts of silt and clay appear to be characteristic of both slope muds and mixed sediments from the slope. Fine-grained shelf sediments commonly contain greater percentages of silt than of clay.

The distribution of sediments on the shelf is patchy and some shelf sediments have textures similar to those on the slope. The end-members of sand and mud may be considered characteristic of shelf and slope environments, respectively, but sediments of intermediate texture occur both on the shelf and the slope.

Sorting: The phi-deviation, a measure of sorting, is plotted as a function of mean grain-diameter in Figure 4. Shelf sand and slope mud form end-members as in Figure 3, with mixed sediments occurring between these extremes. The same symbol is used for individual samples plotted in Figures 3 and 4.

Shelf sands are moderately sorted and slope muds are poorly sorted. Mixed sediments display the poorest sorting.

Mean and Median Grain-Size:--Shelf sands have mean diameters of about 3 phi and slope muds mean diameters of 7 to 9 phi (Table 1). Mixed sediments have mean diameters intermediate to those of sand and mud.

Because the median is less affected by the tails of grain-size distributions, it was used to compare chemical data with sediment texture (Appendix I, Figures 8-18). In general, differences between mean and median diameter are small.

Skewness:--Sandy shelf sediments are positively skewed with phi-skewness values between 0.5 and 0.61 (Table 1). Slope sediments have nearly symmetrical grain-size distributions with skewness values of -0.1 to 0.2, most of which are positive and less than 0.1. Mixed

TABLE 1. Sample locations and sediment size data

Station*	Location		Size Components				Size Statistics**		
	Lat. N.	Long. W.	Sand %	Silt %	Clay %	Sand/Mud <sup>***</sup>	Mean $\phi$	Dev. $\phi$	Skew.
326-28-VV	46°25.6'	124°30.0'	12.7	51.1	36.2	0.2	7.2	3.0	0.1
326-28-00			41.9	28.2	29.9	0.7	6.3	3.3	0.5
326-28-34			14.9	41.6	43.4	0.2	7.4	3.3	-0.0
326-28-42			7.4	43.9	48.8	0.1	7.7	3.1	-0.1
326-28-70			11.2	37.7	51.2	0.1	8.1	3.1	-0.0
326-28-99			3.0	36.6	60.4	0.0			
326-28-145			2.8	38.7	58.4	0.0	8.8	2.3	0.1
326-29-VV	46°26.6'	124°32.4'	35.6	8.0	6.3	6.0	3.0	0.9	0.5
326-29-00			83.2	12.9	3.9	5.0	3.1	1.1	0.4
326-29-40			38.4	42.7	19.0	0.6	5.6	2.8	0.0
326-29-70			64.5	24.4	11.1	1.8	4.6	2.5	0.6
326-31-00	46°31.7'	124°27.5'	1.6	47.3	51.1	0.0	8.1	2.5	0.0
326-31-45			1.5	52.6	45.9	0.0	8.2	2.8	0.2
326-31-88			12.3	45.1	42.6	0.1	7.6	3.0	0.1
326-36-TR	46°29.0'	124°42.4'	11.9	47.2	41.0	0.1	7.3	3.1	0.0
326-36-00			1.2	47.0	51.8	0.0	8.3	2.7	0.1
326-36-50			3.0	51.1	45.9	0.0	7.9	2.9	0.1
326-36-100			2.7	64.2	33.2	0.0	7.8	2.9	0.2
326-36-150			2.1	54.0	43.9	0.0	7.9	3.0	0.1
326-36-200			4.8	60.3	35.0	0.1	7.7	3.2	0.4
326-36-240			1.3	72.6	26.0	0.0	7.4	1.8	0.3
326-36-250			1.7	58.5	39.8	0.0	8.0	2.8	0.3
326-36-290			1.2	55.3	43.5	0.0	7.8	2.9	0.1

\* The first five numbers designate Brown Bear cruise and station, letters VV a Van Veen sample, TR the top of a trigger core, and other numbers the depths of samples in piston cores in centimeters.

\*\* Size statistics (in phi notation) are those of Inman, 1952. (Appendix III).

\*\*\* Mud equals silt plus clay.

TABLE 1 (cont)

Station	Location		Size Components				Size Statistics		
	Lat. N.	Long. W.	Sand %	Silt %	Clay %	Sand/Mud	Mean $\phi$	Dev. $\phi$	Skew.
326-37-TR	46°27.4'	124°39.4'	1.0	50.2	48.9	0.0	8.2	2.2	0.1
326-39-VV	46°20.9'	124°32.7'	83.2	9.7	7.1	5.0	2.7	1.6	0.5
326-42-00	46°23.5'	124°43.8'	0.7	46.5	52.8	0.0			
326-42-50			0.4	53.6	46.1	0.0	8.0	2.7	0.1
326-42-100			0.6	45.7	53.7	0.0	8.5	2.6	0.1
326-42-150			0.6	48.1	51.3	0.0	8.8	2.4	0.3
326-42-175			0.5	45.4	54.1	0.0			
326-44-TR	46°34.0'	125°02.0'	4.5	48.8	46.7	0.1	7.7	2.0	-0.1
326-44-00			30.9	38.0	31.2	0.5	5.7	4.2	-0.2
326-44-30			4.5	51.6	43.9	0.1	7.9	2.3	0.1
326-44-55			0.6	59.2	40.2	0.0	8.0	2.2	0.2
326-45-TR	46°28.0'	124°59.9'	2.5	48.8	48.8	0.0	8.7	2.4	0.3
326-45-00			1.3	50.1	48.6	0.0	8.2	2.5	0.1
326-45-50			0.2	43.9	55.9	0.0	8.7	2.5	0.1
326-45-100			0.4	48.6	51.0	0.0	8.7	2.4	0.2
326-45-130			0.4	45.2	54.5	0.0	8.7	2.6	0.2
326-46-TR	46°23.6'	124°56.8'	1.1	58.2	40.8	0.0	8.0	2.6	0.2
326-46-00			22.6	39.9	37.5	0.3	6.8	3.1	-0.1
326-46-50			0.6	58.6	40.8	0.0	7.8	2.8	0.2
326-46-100			0.5	54.1	45.4	0.0	8.3	2.5	0.2
326-46-145			0.6	54.0	45.3	0.0	8.4	2.2	0.3
326-47-00	46°21.5'	125°11.2'	0.4	60.0	39.6	0.0	7.5	1.8	-0.1
326-47-50			0.8	58.4	40.8	0.0	7.9	1.8	0.2
326-47-100			0.8	56.7	42.5	0.0	7.9	1.9	0.1
326-47-150			0.3	53.6	46.1	0.0	8.1	1.8	0.2
326-47-200			0.4	54.3	45.3	0.0	8.0	1.8	0.1
326-47-234			0.1	55.4	44.5	0.0	8.0	2.1	0.1

TABLE 1 (cont)

Station	Location		Size Components				Size Statistics		
	Lat. N.	Long. W.	Sand %	Silt %	Clay %	Sand/Mud	Mean $\phi$	Dev. $\phi$	Skew.
326-48-00	46°27.0'	125°12.8'	0.9	45.4	53.8	0.0			
326-48-32			9.4	48.2	42.4	0.1	7.7	3.0	0.1
326-48-62			2.2	42.8	55.0	0.0	8.0	3.2	-0.1
326-48-91			38.0	30.1	32.0	0.6	6.6	3.7	0.2
326-48-130			0.9	43.5	55.6	0.0			
326-48-158			1.9	51.6	46.5	0.0	8.4	2.8	0.4
326-48-180			70.4	17.4	12.2	2.4	4.6	2.5	0.7
326-48-190			65.7	22.7	11.5	1.9	4.5	2.6	0.6
326-48-211			5.5	39.6	54.9	0.1			
326-49-00	46°33.4'	125°15.2'	0.7	41.7	57.6	0.0	8.4	2.7	-0.0
326-49-50			0.4	46.1	53.5	0.0	8.3	2.6	0.0
326-49-100			0.2	41.0	58.8	0.0			
326-49-150			0.6	42.3	57.1	0.0	8.7	2.4	0.1
326-49-170			0.4	44.8	54.8	0.0	8.2	2.7	-0.0
326-50-TR	46°27.7'	125°15.0'	1.2	46.3	52.4	0.0	7.5	1.6	-0.4
326-50-52			0.3	51.5	48.2	0.0	8.0	2.8	0.0
326-50-100			2.2	38.6	59.3	0.0	8.7	2.3	0.0
326-50-130			19.5	42.3	38.2	0.2	6.8	3.6	-0.1
326-50-174			1.3	37.8	60.9	0.0	8.5	1.9	-0.1
326-51-TR	46°14.9'	125°24.5'	0.6	36.3	63.0	0.0	8.9	2.1	0.1
326-51-18			0.4	42.4	57.2	0.0	8.7	2.4	0.1
326-51-57			0.6	44.9	54.6	0.0	8.8	2.4	0.2
326-52-TR	46°20.8'	125°34.7'	0.8	39.9	59.3	0.0			
326-52-00			1.6	45.6	52.8	0.0	8.4	2.5	0.1
326-52-50			1.3	50.3	48.4	0.0	8.6	2.5	0.3
326-52-85			1.7	46.5	51.8	0.0	8.3	2.4	0.1
326-52-93			2.2	49.7	48.1	0.0	8.3	2.1	0.2
326-52-126			0.7	50.7	48.6	0.0	8.5	2.5	0.2

TABLE 1 (cont)

Station	Location		Size Components				Size Statistics		
	Lat. No.	Long. W.	Sand %	Silt %	Clay %	Sand/Mud	Mean $\phi$	Dev. $\phi$	Skew.
312-34-01	46°24.3'	124°51.5'	0.8	54.9	44.3	0.0	8.2	2.8	0.2
312-36-VV	46°40.0'	124°36.0'	58.8	28.5	12.6	1.4	5.0	2.2	0.6
312-37-VV	46°39.0'	124°16.0'	69.6	30.4	0.0	2.3	3.9	0.5	0.3
312-39-VV	46°25.0'	124°10.3'	89.0	9.1	1.9	8.1	3.3	0.4	0.5
312-41-01	46°25.0'	124°34.6'	6.3	54.2	39.5	0.1	7.7	3.0	0.2
291-22-VV	46°22.6'	124°09.0'	91.4	7.7	0.9	10.6	3.2	0.4	0.3
291-51-01	46°14.6'	125°29.0'	0.3	55.7	44.0	0.0			
291-53-VV	46°20.7'	124°33.9'	86.4	8.1	5.5	6.4	2.1	1.0	0.4
291-62-00	46°21.8'	124°17.8'	40.4	42.0	17.5	0.7	5.5	2.9	0.3
291-63-01	46°30.0'	124°34.0'	0.4	50.4	49.1	0.0	8.4	2.5	0.2
291-65-01	46°27.0'	125°03.0'	15.7	61.8	22.3	0.2	6.4	2.4	0.1
291-66-01	46°25.7'	124°54.6'	0.3	44.7	55.0	0.0	8.6	2.3	0.2
291-67-01	46°23.3'	124°41.2'	0.4	51.7	47.8	0.0	8.2	2.3	0.1

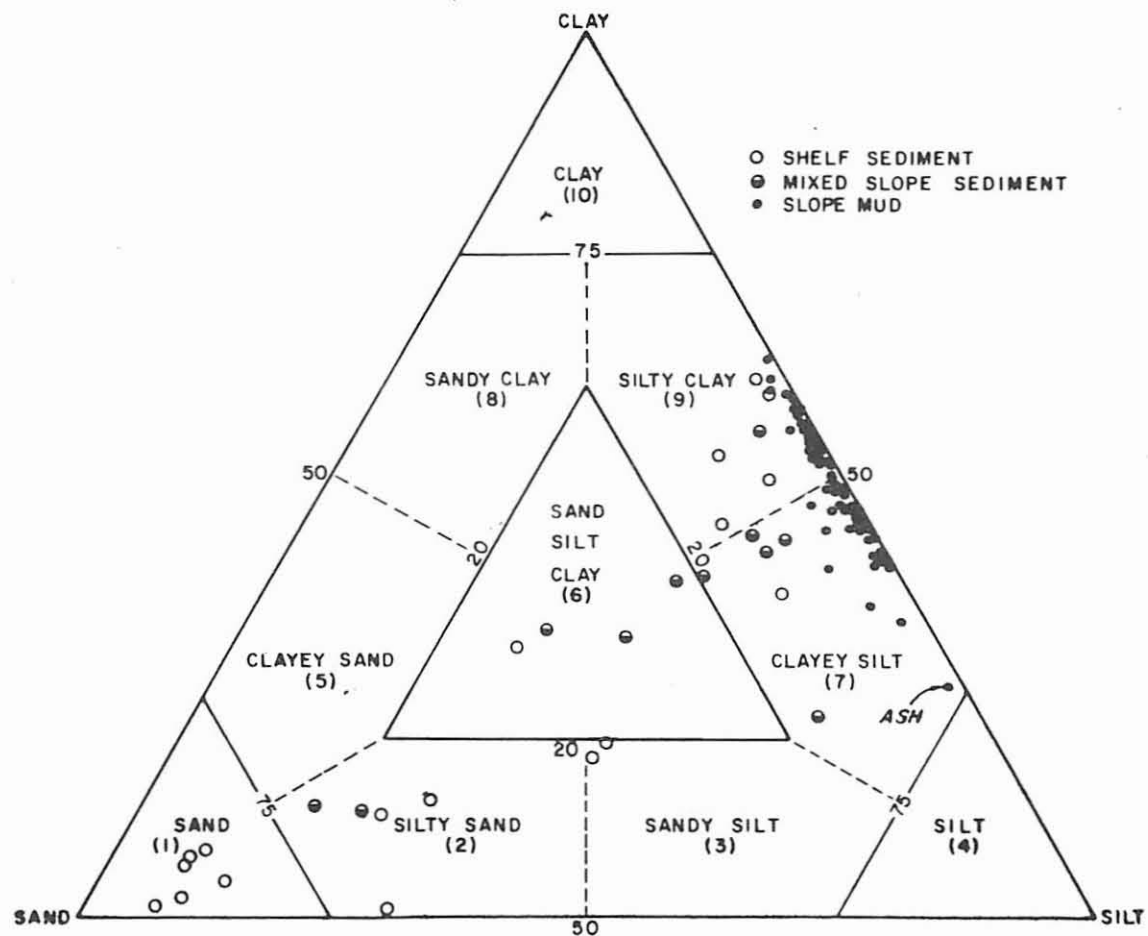


Fig. 3. Sand, silt, clay content of samples.

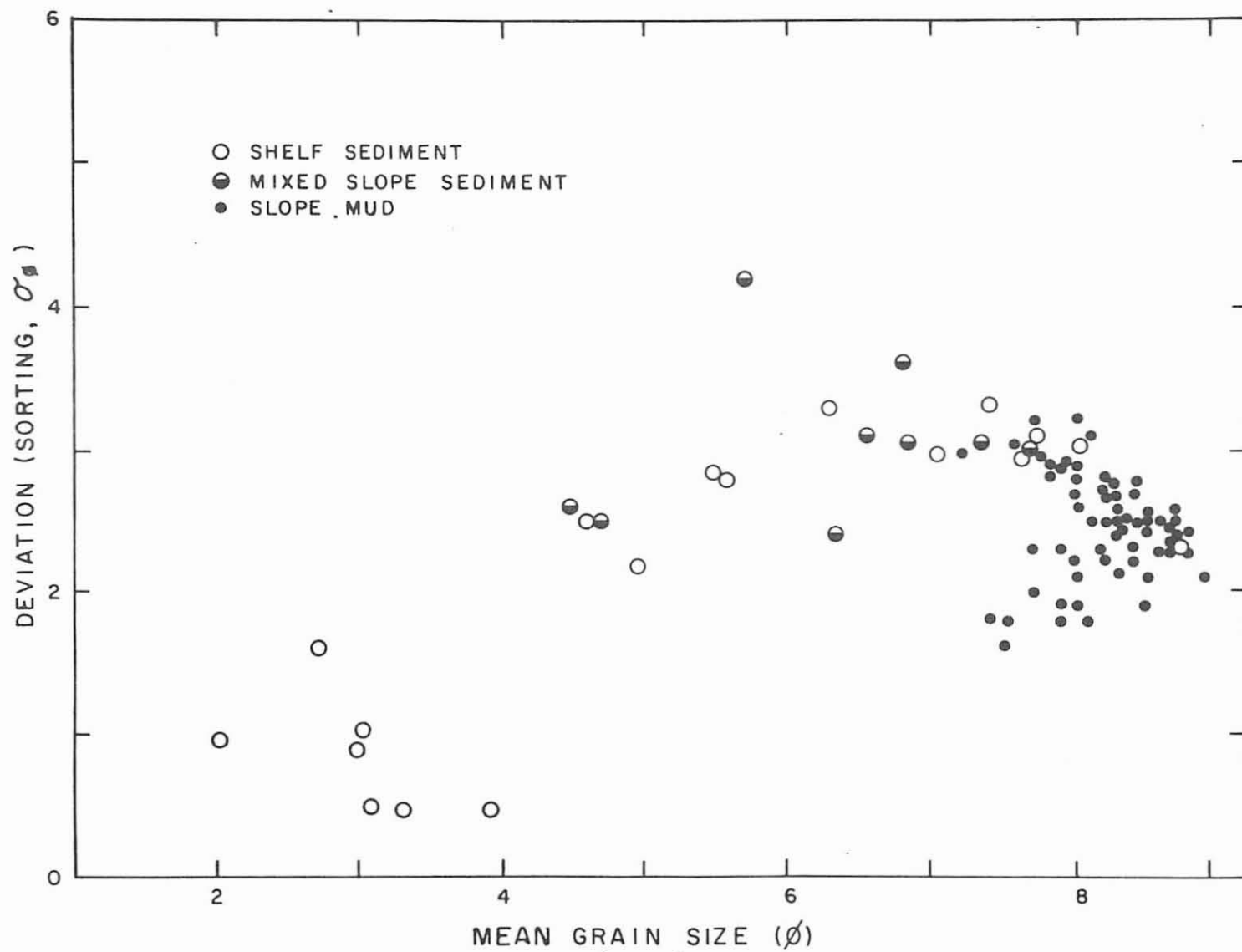


Fig. 4. Sorting as a function of mean grain-size

sediments have skewness values intermediate to those of slope muds and shelf sands.

Carbon and Nitrogen Content:-- Total-carbon (Appendix II) values range from 0.33 to 3.03 per cent, by weight. Calcium carbonate (Appendix II, reported as per cent carbonate-carbon, is relatively low for all samples; seldom exceeding 1.0 per cent and generally less than 0.2 per cent. Organic-carbon contents, estimated by the difference between total-carbon and carbonate-carbon, range between 0.2 and 2.9 per cent. The carbonate-carbon and organic-carbon contents are shown as a function of depth (Appendix I, Figures 8-18) and mean grain-size (Figures 5 and 6).

Coarse-grained shelf sediments contain less carbonate-carbon than slope sediments of similar texture and fine-grained shelf sediments contain more carbonate-carbon than slope muds (Figure 5). High carbonate-carbon contents also occur in fine-grained slope sediments of suspected pre-Holocene age (Figure 5; see Discussion).

An inverse relationship is indicated between mean grain-diameter and organic-carbon content (Figure 6) but a secondary trend of lower organic-carbon values in fine-grained shelf sediments is also suggested. Low organic-carbon contents, correlating with high carbonate-carbon contents, are found in pre-Holocene(?) sediments.

The nitrogen contents, determined by the macro-Kjeldahl method (Appendix II), of eight surface samples from the canyon give organic-carbon/nitrogen quotients between 8.5 and 11.4 which average 9.0.

Water Content:--Water content values were obtained at 10 centimeter intervals in core 326-36. Weighed samples of wet sediment were taken from the core immediately after opening, dried at 90 degrees Celcius, cooled in a desiccator for several hours, and reweighed. Correction was not made for salt content.

Water contents (defined as the ratio of weight of water in a sediment mass to the weight of the oven-dry solid particles) range from 39.5 to 62.2 per cent (Table 2). The maximum deviation of water contents from an eye-fitted regression curve is 3.5 percentage-units except for the value for the ash layer at 240 centimeter depth which plots 7 percentage-units below the regression line.

A coefficient of compaction,  $b$ , was computed (Pettijohn, 1957), using values of water content (per cent by weight) to represent pore space, from the formula,

$$P_z = P_0 e^{-bz},$$

where  $P_0$  represents surface porosity and  $P_z$  the porosity at any depth  $z$ . The coefficient of compaction for core 326-36 is  $5.3 \times 10^{-4}$ .

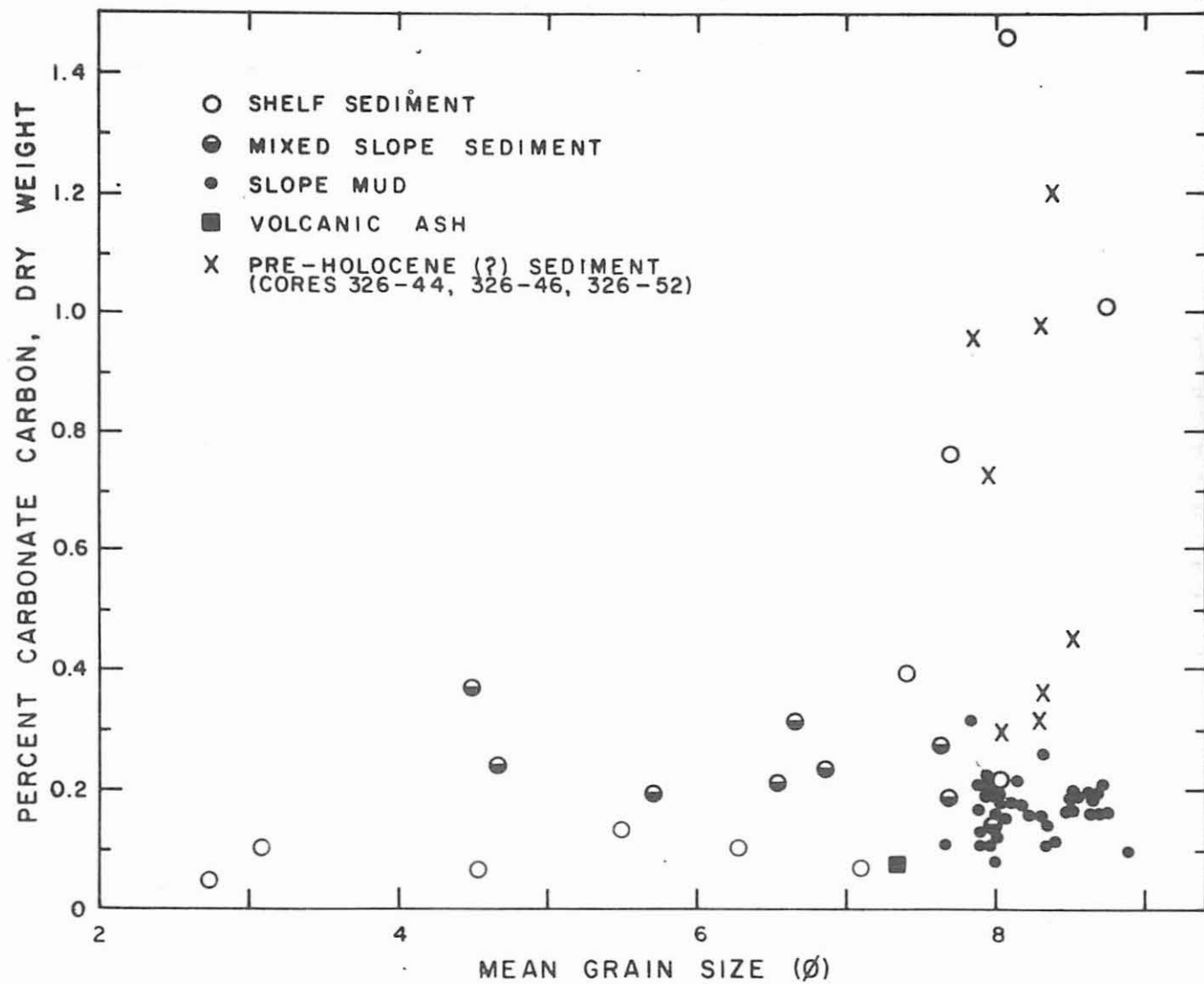


Fig. 5. Carbonate-carbon content as a function of mean grain size.

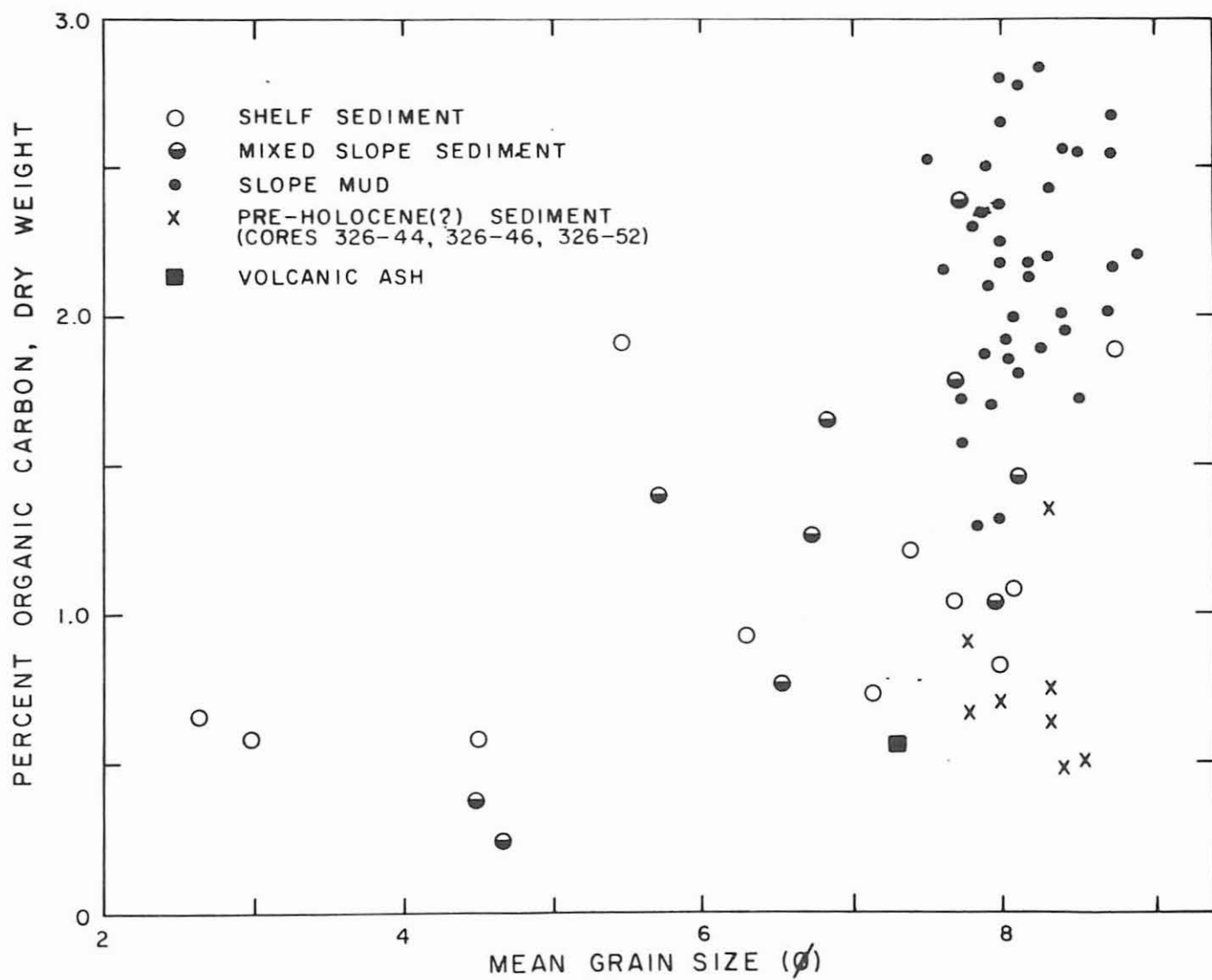


Fig. 6. Organic carbon content as a function of mean grain size.

TABLE 2. Water content of samples from core 326-36

Depth cm	Water %	Depth cm	Water %
10	62.2	160	51.2
20	58.4	170	50.7
30	59.8	180	52.7
40	58.9	190	48.3
50	56.5	200	48.1
60	57.8	210	47.2
70	56.4	220	45.4
80	53.1	230	47.5
90	52.5	240*	39.5
100	58.5	250	46.5
110	55.3	260	46.7
120	51.6	270	45.1
130	51.0	280	44.7
140	51.0	290	43.6
150	53.1		

\*Ash layer

Heavy Mineral Suites:--To compare the composition of shelf sands and sandy sediments from the slope, a petrographic study was made of heavy minerals (densities greater than 2.89 grams per cubic centimeter) in five shelf and four slope samples. Mineral separations were made using the frozen bromoform technique of R. A. MacKay (Fessenden, 1959). A representative portion of each heavy mineral fraction was mounted in Lakeside-70 plastic resin on a glass slide for mineral identification and estimate of composition. The percentage of heavy minerals in the modal size-classes are given in Table 3.

To simplify the task of determining the relative abundances of heavy minerals, they were grouped into classes and the percentage of each class determined (Table 4).

Lithic fragments were mostly basalt with euhedral plagioclase and magnetite inclusions; fragments of siltstone and metamorphic rock composed less than 3 per cent of the lithic component. Volcanic glass was predominantly dark-colored and devitrified but the glass in sample 326-50-130 was red-brown.

Opaque minerals include magnetite, ilmenite(?), and some dark, volcanic glass. Clinopyroxines were chiefly augite but some diopside was observed. Brownish-green hornblende was the most common amphibole but a blue-green variety was often present and was abundant in samples 326-29-00 and 326-50-130. Hypersthene, which frequently showed

TABLE 3. Heavy-mineral percentages, by weight, of selected samples from the canyon rim and lower canyon

Sample	Heavy minerals	
	2 $\phi$ -class	3 $\phi$ -class
326-29-VV	11.37%	3.03%
326-29-00	12.30	10.03
326-29-40	8.70	9.28
326-29-70	12.50	10.40
326-39-VV	33.61	29.16
326-48-90		7.31
326-48-180		4.32
326-48-190		9.69
326-50-130		8.77

solution along terminal margins of prismatic crystals, was the dominant orthopyroxine, but minor amounts of enstatite were noted.

Micas included chlorite, biotite, and colorless mica; some colorless mica may be leached biotite. Pink, amber, and brown garnets were most common; some orange and green garnets were present. Green or yellow-green to whitish epidote showed signs of sericitization.

Grain shape varied among the constituents. Orthopyroxines and amphiboles were generally euhedral to sub-hedral and sub-rounded. Volcanic rock fragments were sub-rounded to sub-angular. Clinopyroxines were euhedral and sub-angular to angular, and glass and opaque minerals were rounded to sub-rounded.

Light-Mineral Suites:--The light-mineral fraction (density less than 2.89 grams per cubic centimeter) was composed principally of equant grains of sub-angular quartz with minor percentages of unaltered plagioclase-feldspar. The content of volcanic glass, lithic fragments, glauconite, and foraminifera varied among the samples. Diatoms, radiolaria, sponge spicules, echinoid spines, fish teeth and vertebrae, and algal debris were minor biogenous constituents.

Glauconite, distinguished by its morphology and dark green color (Burst, 1958), and volcanic ash were noted in many samples examined for foraminifera. Glauconite was most abundant in sand from the outer shelf and in coarse fractions of sediments near the shelf break. In contrast, volcanic ash was most abundant in fine-grained sediments from the lower canyon. Ash and glauconite were observed at all depths in cores.

TABLE 4. Heavy mineral compositions of selected samples from the canyon rim and lower canyon\*

Mineral Group	Samples from <u>Brown Bear</u> cruise 326									
	29-VV	29-00	29-40	29-70	39-VV	45-90	48-130	48-190	50-130	
Lithic fragments	63%	49%	70%	66%	63%	75%	74%	73%	58%	
Volcanic glass	11	13	7	4	4	8	5	5	13	
Opaque minerals	8	4	8	11	15	5	5	15	7	
Clinopyroxines	9	7	6	8	7	4	7	3	8	
Amphiboles	4	13	4	6	3	2	5	2	5	
Orthopyroxines	3	4	1	3	5	1	1	1	4	
Mica	1	6	4	2	-	4	2	1	4	
Epidote	Tr	2	-	-	1	-	Tr	-	-	
Garnet	Tr	1	Tr	Tr	-	-	Tr	-	-	
Monazite	Tr	-	-	-	-	-	-	-	-	
Sphene	-	1	-	-	1	-	-	-	Tr	
Zircon	-	-	-	-	-	-	Tr	-	Tr	
Pyrite	-	-	Tr	Tr	-	-	Tr	-	Tr	
Sillimanite	-	Tr	-	-	-	-	-	-	Tr	
Kyenite	-	-	-	-	-	Tr	-	-	Tr	

\* Percentages determined by counting 300 grains.

Tr Mineral concentrations less than one percent.

- Minerals not detected.

The average refractive index of the volcanic ash from the layer at 240 centimeters depth in core 326-36 (Appendix I, Figure 10) was 1.505. X-ray diffraction identification of the crystalline components of the ash was impossible because of their low concentrations and contamination of the ash layer by other lithogenous material.

Clay Minerals:--Identification of clay minerals (Appendix II) was based on the orderly repetition of the X-ray diffraction peaks from the basal (001) crystallographic lattice. The clay-mineral suite consisted of mica-species, referred to as illite, characterized by 10 Angstrom and 5 Angstrom X-ray diffraction peaks; kaolinite; Fe-chlorite; montmorillonoids; and mixed-layer structures.

Estimates of the relative abundances of illite, Fe-chlorite, and kaolinite were obtained by comparing the areas of major diffraction peaks before and after acid treatment. Ratios of 7.1A/10A and 3.5A/3.3A peak-areas were considered a measure of Fe-chlorite + kaolinite/illite before acid treatment and kaolinite/illite after acid removal of Fe-chlorite. The value of the 7.1 Angstrom diffraction peak was divided by two to adjust for the relative intensity of the 10 Angstrom peak (Weaver, 1958). Peak ratios and illite: Fe-chlorite:kaolinite ratios computed by this method are given for surface samples in Table 5. Values of the 4.7A/5.0A ratio are also recorded. Additional peak ratios for three cores are shown in Table 6.

Foraminifera:--An effort was made to obtain samples for foraminiferal study from the tops of trigger (short gravity) cores but in several cases it was necessary to use the tops of piston cores. Samples were wet-sieved through a 4-phi (62-micron) screen, stained with Rose Bengal dye, and sized into single phi-unit classes. Identifications were made by B. J. Enbysk<sup>1</sup> of the Department of Oceanography, University of Washington.

The distribution of foraminifera in surface samples is shown in Table 7 and in selected cores in Table 8. Sample locations are shown in Figure 2<sup>2</sup>.

<sup>1</sup> A discussion of foraminiferal zonation off the Washington coast, including Willapa Canyon, is being prepared by B. J. Enbysk and will be available in the near future.

<sup>2</sup> The locations of three samples from Cascadia Basin, west of Willapa Canyon, not shown in Figure 2 are: 312-34 (Lat 46°24.3' N, Long 125°51.5' W); 312-56 (Lat 46°14.5' N, Long 126°00' W); and 291-50 (Lat 46°12.1' N, Long 126°20.8' W).

TABLE 5. Intensity ratios of major X-ray diffraction peaks of surface samples before and after acid treatment and their estimated illite:Fe-chlorite:kaolinite ratios (see text for explanation)

Station	Peak-area ratios before and after acid treatment						Illite:Fe-chlorite:kaolinite	
	4.7A/5.0A		7.1A/10A		3.5A/3.3A		computed from	
	before	after	before	after	before	after	3.5A/3.3A	7.1A/10A
326-28	0.5	0.3	1.2	0.6	0.5	0.3	10:2:3	10:3:3
326-29	0.9		2.3		0.8			
326-31	1.0	1.0	1.0	1.0	0.8	0.5	10:3:5	10:5:5
326-36	1.0	0.6	1.2	1.0	0.5	0.4	10:1:4	10:1:5
326-37	1.0	0.6	2.0	1.0	0.6	0.3	10:4:3	10:5:5
326-39	0.5	0.5	1.0	1.0	0.7	0.7	10:0:7	10:0:5
326-42	1.5	0.5	1.6	1.0	1.0	0.8	10:3:7	10:4:5
326-44	1.0	0.2	3.0	0.5	0.7	0.2	10:5:2	10:12:3
326-45	0.1	0.6	2.4	1.0	0.8	0.5	10:3:5	10:7:5
326-46	0.6	0.2	0.5	0.5	0.5	0.3	10:2:3	10:1:2
326-46*	1.0	0.5	1.0	0.8	0.8	0.4	10:4:4	10:1:4
326-47	1.0	0.4	2.0	2.0	0.7	0.5	10:2:5	10:0:10
326-48	1.0	0.5	1.6	1.0	0.8	0.5	10:3:5	10:3:5
326-49	1.0	0.7	1.3	1.0	0.7	0.5	10:2:5	10:2:5
326-50	1.0	0.3	1.0	1.0	0.8	0.6	10:2:6	10:0:5
326-51	1.0	0.5	1.7	1.0	0.8	0.4	10:4:4	10:4:5
326-52	1.0	0.2	1.5	1.0	0.8	0.2	10:6:2	10:3:5

\* Sample from top of trigger core

TABLE 6. Intensity ratios of major X-ray diffraction peaks for the clay-size sediment in untreated samples from four cores

Sample*	Ratio of major peak-areas			Sample	Ratio of major peak-areas		
	4.7A/5.0A	7.1A/10A	3.5A/3.3A		4.7A/5.0A	7.1A/10A	3.5A/3.3A
326-28-00	0.9	2.3	0.5	326-48-00	1.0	1.6	0.8
326-28-34	1.0	2.0	0.3	326-48-32	1.0	1.0	0.9
326-23-42	0.6	1.1	0.5	326-48-62	0.8	1.3	1.0
326-28-70	0.5	2.0	0.8	326-48-91	1.0	1.7	0.6
326-28-99	1.0	1.1	0.8	326-48-130	1.0	1.3	0.8
326-28-145	1.0	1.2	0.7	326-48-158	1.0	1.5	0.9
				326-48-180	0.7	1.2	0.5
326-36-00	1.0	1.2	0.5	326-48-190	1.0	1.5	1.0
326-36-10	1.0	1.2	1.8	326-48-211	1.3	1.6	0.8
326-36-50	0.8	1.6	0.9				
326-36-100	1.0	1.1	1.0	326-52-00	1.0	1.7	0.7
326-36-150	1.0	1.1	0.7	326-52-50	1.0	1.5	0.8
326-36-200	1.0	1.2	0.5	326-52-85	1.0	2.4	1.0
326-36-240**	1.5	1.0	0.8	326-52-93	1.5	1.8	0.6
326-36-250	1.0	1.2	0.8	326-52-126	1.0	1.3	0.6
326-36-290	1.0	1.0	0.9				

20

\* The first five numbers designate Brown Bear cruise and station, and other numbers the depths of samples in piston cores in centimeters

\*\* Ash layer

## LEGEND FOR FORAMINIFERA TABLES

Samplers

VV	Van Veen
GC	Gravity corer
Ku	Kullenberg corer
Tr	Trigger core of Kullenberg corer
Dr	Dredge

Locations

Sh	Shelf above canyons
G	Guide Canyon
W	Willapa Canyon
U	Upper Canyon to 125° W
L	Lower Canyon 125° to 126° W
O	Outer Canyon beyond 126° W
RB	Right Bank (facing downslope)
LB	Left Bank
Ch	Channel (axis)

Sediment Class

Numbers correspond with Shepard (1954)  
Diagram of size classification (Figure 3)

Abundance Notations

Z	Ooze (greater than 30 percent biogenous material)
A	Abundant
C	Common
R	Rare
F	Few
/	Present
v	varied - many genera

Minor Elements

A	Ash
F	Fossil (pre-Holocene materials)
Fi	Fish bones or teeth
G	Glauconite
Mo	Mollusca
My	Mysid statocysts
O	Ostracods
P	Pellets
Py	Pyrite
Sp	Sponge spicules
S	Sand

Foraminifera Species

O	Living specimen present
△	Displaced

Numbers in parentheses refer to biotypes, micropaleo collection,  
Department of Oceanography, University of Washington.











TABLE 8

## SUMMARY OF FORAMINIFERA IN SELECTED CORES

## WILLAPA CANYON

CORE (C-14 date)	Interval in cm.	Class	Diatoms	Radiolaria	Globigerinids	Aren/gm	Aren. spp.	Calc./gm	Calc. spp.	Displaced/gm	Displaced spp.	Accessory	COMMENTS
312-56 GC	0-5	9	F	R	/	1	2	5	13	0	0	P	Little change in numbers of displaced species or individuals. Abundance of globigerinids variable in past 5000 years. Typical decrease in arenaceous species and numbers in lower intervals.
1400fm	3-5	9	R	R	/	3	7	6	19	0	0	P	
Outer Channel	10-12	9	R	C	F	2	8	6	27	1	2		
(4300	20-22	9	R	F	/	1	3	3	11	1	3	Py	
+300	40-42	9	F	R	F	2	6	8	25	2	4	P	
E.P.)	52-54	7	F	R	/	1	1	1	11	1	3	A	
	80-82	9	R	C	R	1	2	5	31	1	4	A,Py	
	(94-96)	7	R	C	F	1	2	9	31	2	5	A,Py,P	
326-48 Ku	0-5	9	/	R	/	14	18	12	19	1	2	S	Great variation in numbers of displaced species and individuals and total foraminiferal numbers. Evidently some size-weight sorting of species so that 3 and 4 sizes greatly increase <u>Epistominella pacifica</u> counts. Few shelf displaced species. Majority of displacements from upper and middle bathyal.
1123fm	31-33	7	/	F	O	0	0	40	22	16	6	S	
	62-64	9	F	Rv	/	12	3	50	30	27	7	S,A,My	
Lower Channel	88-90	6	/	/	O	6	2	100	35	60	10	S,A,Py	
	128-130	9	F	Rv	F	2	4	15	29	3	8	O	
	158-160	7	F	/	/	1	2	7	6	6	8	Py,S	
	178-180	2	/	/	/	1	2	100	36	60	15	S,A,Py	
	188-190	2	/	/	/	1	3	36	26	30	20	M,S,A,Py	
	209-211	9	/	/	/	2	3	28	16	27	10	S,A,Sp,Py	
326-52 Ku	Top	9	F	Rv	O	3	8	4	6	0	0	A,S	Lower interval poorly preserved, possibly pre-Holocene.
1033fm Left Bank	124-126	7	/	/	F	0	0	4	7	3+	4	Py	
326-51 Ku	Top	9	F	Fv	O	1	6	3	4	1	1		Interval 56-58cm has shoaler aspect (approx. 200 fm) in addition to species displaced from shelf.
850fm	17-19	9	/	Rv	/	2	2	7	23	1	2	A	
Left Bank	56-58	9	/	/	/	1	3	16	13	4	3		
326-46 Ku	Top	7	O	/	O	2	4	11	6	2	2	S	Below surface intervals are probably pre-Holocene indicated by <u>Cibicides mckannai</u> , <u>Cassidulina teretis</u> , and <u>Cassidulinoides mexicana</u> and greatly increased displacement.
700fm	0-5	6	/	Fv	/	2	4	12	14	1	1	Py	
Left Bank	50-52	7	/	/	R	0	0	20	10	3	3	Py	
	100-102	7	/	/	C	0	0	100	33	50	7	Py,O	
	145-147	7	/	/	C	0	0	100	36	40	7	Py	
326-36 Ku (1677)	Top	7	/	/	O	1	3	24	17	1	1	A,My	Essentially barren interval above ash layer. Some solution of tests in ash layer. Deeper aspect of intervals below ash suggested by abundant <u>Gyroidina altiformis</u> and increased globigerinids.
360fm +120)	(0-5)	9	/	/	/	1	1	35	21	1	1	Py,A	
(4860	50-55	7	/	Rv	O	0	0	40	7	0	0	Py	
+200	100-105	7	F	/	O	0	0	11	7	0	0	Py	
Right Bank	(150-155)	7	F	F	O	0	0	15	8	0	0	Py	
(7754	200-205	7	/	Rv	O	0	0	1	1	0	0		
+300)	239-241	7	/	/	/	0	0	17	10	1	2	A,Py	
	(250-255)	7	F	F	/	0	0	75	18	1	1	A,Py	
	285-290	7	/	/	F	0	0	33	22	1	2	Py	

Wall Rock

Consolidated sedimentary rock, dredged from the canyon walls at station 326-33, consisted of an indurated, gray siltstone which becomes somewhat friable on drying. Hand-sized specimens were randomly fractured and colored buff to red and brown along exposed surfaces. Some specimens were thinly bedded. Selected fragments were cleaned and disaggregated for micro-fossil and mineral examination. Approximately 25 per cent of the disaggregated rock was coarser than 4 phi (62 microns).

The major constituents of the coarse fraction (coarser than 4 phi) in order of abundance were quartz, lithic (basaltic and andesitic) fragments, mica (chloritic), and feldspar. Minor amounts of garnet and zircon were present. Because cracks and burrows in the wall rock were filled with Holocene material, minerals present in trace amounts were not listed as part of the wall-rock mineral suite. The wall rock matrix, determined by X-ray diffraction analysis, consisted mostly of illite and kaolinite.

Foraminifera from disaggregated material were examined by B. J. Enbysk, University of Washington; G. F. Fowler, University of Oregon; and O. L. Bandy, University of Southern California. Of the many species present, seven or eight may be fossil forms (Table 7). Although the evidence is tenuous, Bandy and Fowler estimated their age to be Lower Pliocene (B. J. Enbysk, personal communication); Enbysk (personal communication) believed that none of the species were distinctive but agreed that the material appears old and an age of Pliocene is reasonable. No planktonic foraminifera were observed. Some radiolaria were present.

Cohesive clayey-silt dredged at station 326-38 may be of pre-Holocene age but fossil evidence is lacking. No rock was obtained from station 326-41.

Depositional Rates

Three carbon-14 dates<sup>3</sup> obtained for intervals near the top, middle, and base of core 326-36 by the total organic-carbon method are given below.

Upper core	(0-19 cm)	1677 ±120 years B.P.
Middle core	(132-150 cm)	4860 ±200 years B.P.
Lower core	(250-265 cm)	7754 ±300 years B.P.

The dates were applied to the midpoint of the core interval dated.

The average specific gravity of solid particles (Krumbein and Pettijohn, 1938, p. 680) in four sub-samples from the core was found

<sup>3</sup>Radiocarbon dates were obtained from Isotopes, Inc., 123 Woodland Avenue, Westwood, New Jersey.

to be 2.53 grams per cubic centimeter. This value was used with the average dry-bulk densities (dry-sediment weight per unit volume in the core) of the intervals between carbon-14 dates to compute depositional rates. The rates obtained were:

Upper core	(10-140 cm)	45.7 mg cm <sup>-2</sup> yr <sup>-1</sup>
Lower core	(140-257 cm)	53.6 mg cm <sup>-2</sup> yr <sup>-1</sup>
Average	(0-257 cm)	49.7 mg cm <sup>-2</sup> yr <sup>-1</sup>

The rate of sedimentation expressed as length per time is rather inexact (Koczy, 1963) and the unit of mass/area per unit time is preferable because it is independent of sediment compaction and water content. The average depositional rate expressed as length per time is about 41 centimeters per thousand years.

The depositional rates of sediment components can be estimated as the product of their abundance and the average depositional rate. Values for core 326-36 are given in Table 9.

TABLE 9. Estimated depositional rates of sediment components in core 326-36

Sediment component	Depositional rate mg cm <sup>-2</sup> yr <sup>-1</sup>
CaCO <sub>3</sub>	0.8
Organic matter	2.2
Lithogenous matter	47.0
Total	50.0

The carbonate rate was obtained from the average carbonate content of the core. A value of organic content was obtained by multiplying the total nitrogen content (average of two analyses) at the surface by a factor of 17 (Emery, 1960).

## DISCUSSION AND INTERPRETATION

### Description of Sediments

Well sorted sands dominate the outer shelf adjacent to Willapa Canyon and green pelagic muds predominate within the canyon. The muds are layered accumulations with discontinuities at intervals of about 10-30 centimeters.

Wet cores show only minor variations in color, the dominant hues being grey-green (5Y3/2 - 5Y4/2) to olive green (5GY4/2) (Appendix I, Figures 8-18). Variation in grain-size and mineralogy may account for color changes but minor differences of color are not readily related to sediment composition. According to Grim (1951) and Keller (1953) illite and montmorillonoids cause the green color of many shales (Emery, 1960). In Willapa Canyon, Fe-chlorite probably contributes appreciably to the green color of the sediment. Glauconite may also color the shelf sands but it is doubtful that it is significant in the slope muds. No systematic color change was noted (consistently) either areally or with depth in the wet cores.

Obvious textural changes, such as sand layers, characterize only a small number of discontinuities (Appendix I, Figures 8-18), and X-radiographs of cores revealed numerous discontinuities not detected in visual inspection of wet cores. Different rates of drying of sediment layers may be related to Fe-chlorite and mixed-layer clay contents, but further study is needed to clarify the relationship. Color changes and differential desiccation in dry cores correlated with subtle density changes noted in X-radiographs.

#### Source of Sediments

Lithogenous Material:--The Columbia River (Figure 2) appears to be the major source of unconsolidated sediment in the vicinity of Willapa Canyon. Ballard (1964) reports that sands along the coast north of the river mouth have a mean grain size of 2.5 phi and Inman sorting values of 0.5-0.6 phi, textures similar to those found on the outer shelf adjacent to Willapa Canyon (Table 1).

Sediments from the inner shelf east of Willapa Canyon have heavy mineral compositions similar to those of the outer shelf (C. F. Royse, unpublished). High percentages of volcanic rock fragments, euhedral hypersthene, and magnetic minerals characterize sediments of both areas. Beach sands north of the Columbia River show similar compositions.

Sediments north of the Columbia River contain more than 40 per cent heavy minerals and large amounts of magnetic minerals (Ballard, 1964). According to Ballard, increased amounts of heavy minerals also occur in beach sands near the entrances of Willapa Bay and Grays Harbor, but the magnetic-mineral contents of these sediments are low. Because the amount of heavy minerals and magnetic minerals decreases with distance from the river mouth, Ballard concluded that the Columbia River is the major source of sand along the beaches of the southern Washington coast. Observation that the beach north of the river mouth is prograding (Ballard, 1964) affirms that sediment is available for offshore transport, and the similarity of texture and composition of inner-shelf, outer-shelf, and nearshore sediments suggests that the Columbia River is also the source of sand on the outer shelf.

Clay-silt sized material probably originates as degradation products of rock in adjacent continental regions and is transported to the shelf by westward flowing streams. The sediment-laden plume of the Columbia River usually extends across the shelf in a southwesterly direction during the spring and fall (seasons of maximum discharge), but it extends north of Willapa Canyon during part of the year. Fine-grained sediment settling from the surface waters of the Columbia River plume might be carried northward by the Davidson Current; a sub-surface, counter-current believed to exist off the Washington coast much of the year (Sverdrup, Johnson, and Fleming, 1942, p. 725).

Trace amounts of well rounded, frosted quartz grains were observed in samples from the outer shelf, but because onshore winds dominate the Washington coast, it is unlikely that a significant portion of outer shelf or slope sediment was wind transported. These grains may represent sediment derived from older strata which is undergoing a second cycle of deposition.

Illite, Fe-chlorite, and kaolinite were present in detectable amounts in nearly all samples, but pre-Holocene(?) sediments contain little or no Fe-chlorite (Figure 7). The illite content appears to vary little while concentrations of Fe-chlorite and kaolinite show minor fluctuations. The uniformity in composition of the clay-sized sediments suggests a single source for clay minerals in the vicinity of Willapa Canyon. Montmorillonoids were present in trace amounts in only a few samples, and were a minor constituent only in core 326-36.

Although the illite:Fe-chlorite:kaolinite values show considerable variation (Table 5) the general relationships are in agreement and suggest that an average clay composition consists of about 20 per cent Fe-chlorite, 30 per cent kaolinite, and 50 per cent illite. Because slope sediments are composed of about 50 per cent clay-sized material by weight (Figure 3), these values correspond to a sediment composition of 10 per cent Fe-chlorite, 15 per cent kaolinite, and 25 per cent illite. This estimate assumes that these minerals are the only clay-sized constituents and, because montmorillonoids and mixed layer clays are present in minor concentrations, the estimate is slightly large.

Griffin and Goldberg (1963, p. 740) state: "The North Pacific coastal deposits show an enrichment in a 'montmorillonite-type' mineral which shows evidence of being composed mostly of expandable stripped illite or chlorite. Such clays probably have as their source the coastal continental areas and are mainly transported to the oceans by water paths." This generalization is not substantiated by analysis of sediments from Willapa Canyon. Disregarding possible effects of differential flocculation and deposition, if montmorillonoids are derived from coastal continental areas, they should be present in the sediments of Willapa Canyon.

Griffin and Goldberg also observe a decrease in chlorite from high latitude regions southward. Results of the X-ray diffraction study (Tables 5 and 6) agree with the high 7.1A chlorite + kaolinite/10A

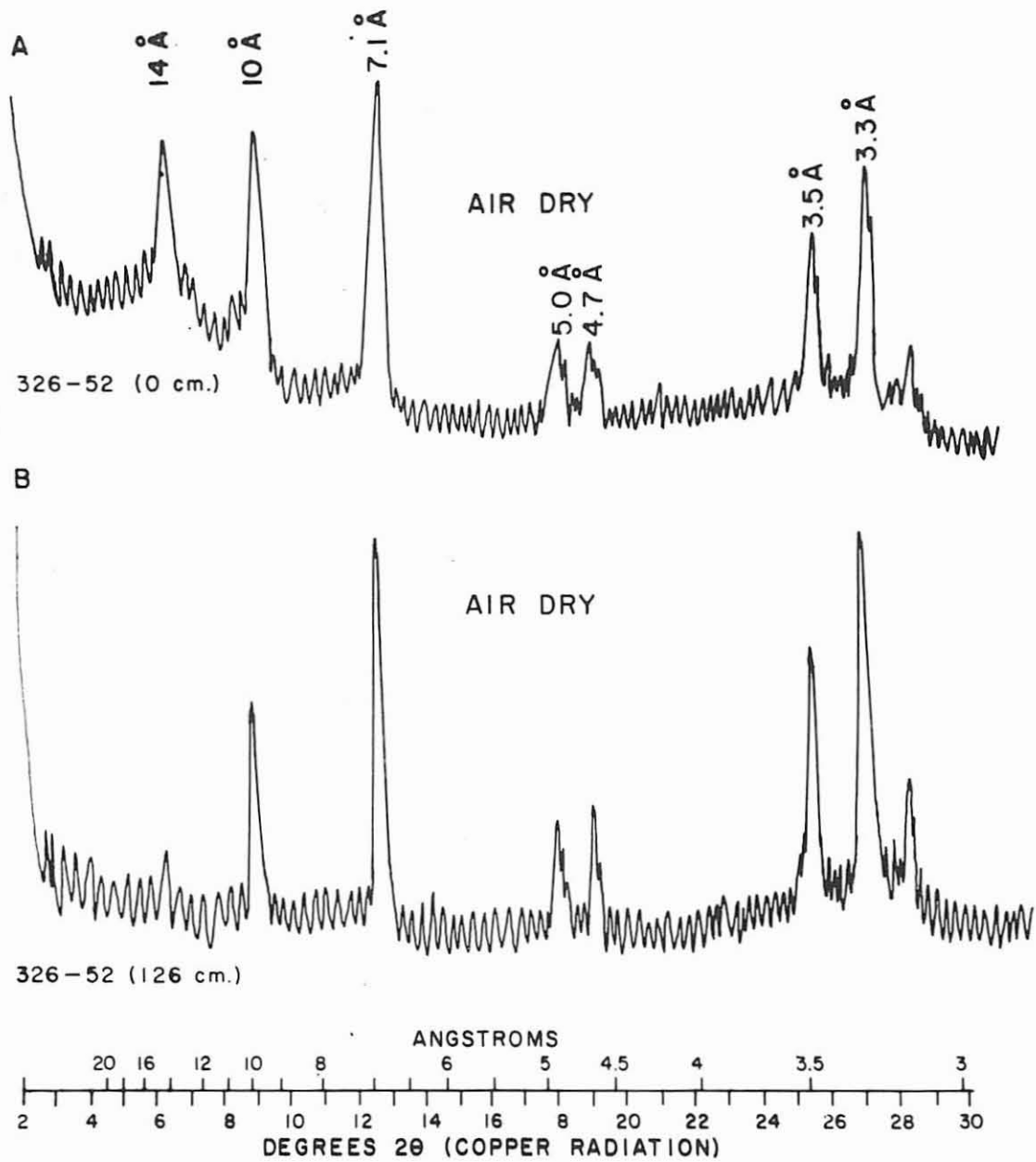


Fig. 7. X-ray diffractograms of samples from core 326-52.

illite ratios ( $>1$ ) obtained by these workers, but in Willapa Canyon the high ratio results from sediment compositions in which the kaolinite content exceeds that of Fe-chlorite. X-ray diffractograms of acid and heat treated sediments also indicate that the 4.7 Angstrom peak results from both Fe-chlorite and kaolinite, a factor not generally noted by many workers (Griffin and Goldberg, 1963; Weaver, 1958). The presence of a strong 4.7 Angstrom peak in the untreated sample 326-52 (Figure 7, B), which contains no Fe-chlorite, supports the conclusion derived from treated samples.

Various workers (Grim, 1951, 1953; Keller, 1953) have attempted to relate clay mineral composition to the environment of deposition, but complicating factors of sediment source, rate of deposition, differential flocculation and deposition, and the low precision of determining clay-mineral composition greatly limit these interpretations. The Willapa Canyon area is probably too small to exhibit changes in clay mineralogy resulting from selective sorting processes. The moderately high rate of sediment deposition and proximity to a terrestrial source is reflected in the high Fe-chlorite and kaolinite content of these sediments. The short residence time of sediments on the slope allows insufficient time for authigenetic changes which presumably increase the amount of illite in marine sediments (Griffin and Goldberg, 1963).

Organic Matter:--The inverse relationship of organic-carbon and grain-size (Figure 6) can be explained as a result of removal of organic matter and fine-grained lithogenous particles by winnowing or more complete oxidation of organic matter in permeable, coarse-textured sediments. The trend of low organic-carbon contents of fine-grained shelf sediments, which contain higher percentages of sand than slope sediments with similar mean grain-diameters (Table 1), can be explained in the same manner.

Trask (1939, p. 445-446) estimated the average organic content of shelf sediments to be 2-3 per cent, and of North Pacific oceanic sediments to be about 1.0 to 1.5 per cent. Concentrations measured at the base of the continental slope off Washington and North Carolina (Trask, 1939, p. 446) were two to three times as large as those on the adjacent shelf. Emery (1960) reported high organic-matter percentages, locally exceeding 10 per cent, for the basins off southern California, and Emery and Hulsemann (1963) found an average total organic matter content of about 2.0 per cent for 13 canyons off southern California; a value greater than that of adjacent shelf sediments and less than that obtained for adjacent basin sediments.

The average carbon-nitrogen ratio for surface sediments of Willapa Canyon is 9.0 and, although the number of determinations is small, it is believed to be representative of the area.

Trask (1939) obtained a ratio of 8.4 for 86 surface samples from the Channel Islands off southern California. Subsequent analyses by Emery (1960) of samples from the same area gave a mean value of 12.2. The difference is accounted for in part by the fact that some of Emery's samples were obtained at depth in cores. An average of surface

values alone gave a ratio of 11.2, and Emery (1960, p. 276) accepts a carbon-nitrogen value of 10 as representative of the area. Lower ratios are reported for basin sediments off southern California, averaging about 8.0 (Emery, 1960). The value of 10 is identical with the ratio for soils (Waksman, 1931) and for sediments of the north Baltic Sea (Gripenberg, 1934). Gucluer (1962) obtained a value of 10.5 for sediments from Saanich Inlet, British Columbia; Anderson (1962) a value of 10.1 for sediments of Deep Inlet, Alaska; and Bader (1955) a ratio of 9.1 for sediments from a Maine fjord. Emery and Hulsemann (1963) found an average carbon-nitrogen ratio of 8.9 for sediments from canyons off southern California, a value nearly equal to that of Willapa Canyon sediments.

Marine organisms generally have higher nitrogen contents than terrestrial plants, resulting in lower carbon-nitrogen ratios; but the variable composition of organic matter and different rates of decomposition will affect the ratio measured in a sediment. Trask (1932), Bader (1955), Emery (1960), and others discuss control of the carbon-nitrogen ratio by the type of organic material deposited, its rate of decomposition, and associated sediment types. It appears that use of the ratio as an index of depositional environment is limited, but Scholl (1963) has demonstrated that the ratio for swamp sediments in southwestern Florida is controlled by the type of organic material being deposited. The high ratios (about 13) obtained for shelf sediments adjacent to the swamps indicate that terrestrial organic material is reaching the outer shelf in sufficient quantity to alter the carbon-nitrogen ratio established by planktonic and benthic organisms.

Organic matter in Willapa Canyon sediments is probably derived from planktonic marine organisms. The possibility of major contributions from land sources can be disregarded, but algal debris observed in some samples indicate that some organic material originates in the eulittoral environment.

Calcium Carbonate:--The relationship between grain-size and carbonate-carbon content (Figure 5) is not consistent. The sandy sediments from the outer shelf are low in carbonate-carbon compared to coarse-grained sediments in cores from the lower canyon. The high carbonate-carbon values in sands from the slope result from concentrations of fragmented, bivalve shells and pyrite-filled, foraminiferal tests. Variations in carbonate-carbon percentages in fine-grained, slope sediments (Appendix I, Figures 8-18) correlate with numbers of calcareous foraminifera (Table 8), indicating that these organisms are the major source of carbonate in slope sediments. Pre-Holocene(?) sediments (cores 326-44, 326-46, and 326-52) contain more carbonate-carbon than do Holocene slope sediments. In core 326-46 the high carbonate-carbon content correlates with concentrations of calcareous foraminifera (Table 8), but in core 326-52 this relationship is not evident. The high carbonate-carbon contents of pre-Holocene(?) sediments appear to result from factors other than concentrations of calcareous organisms.

### Pre-Holocene Sediments

Silty clays in cores 326-44, 326-46, and 326-52 have low organic-carbon contents (Figure 6), high carbonate-carbon contents (Figure 5), low Fe-chlorite contents (Figure 7), and contain abundant blue, iridescent pyrite. These characteristics are anomalous compared to those of other fine-grained sediments from the slope and are interpreted as indications that the sediments are not of Holocene age.

Diagnostic index fossils have not been found in these sediments but work in progress (B. J. Enbysk, Department of Oceanography, University of Washington) indicates that the specific relationships of foraminiferal assemblages in these sediments are different from those of Holocene sediments (Table 7). Evaluation of these relationships is complicated by the possibility of displacement in the fossil faunas. It is hoped that further study will give more definite indications of the age of these sediments.

The frequent recovery of pre-Holocene(?) sediments in cores from the lower canyon area suggests that the lower slope is essentially a region by-passed by sediment with only a thin cover of Holocene sediment.

Consolidated sediment was obtained in the dredge haul from the north wall of Guide Canyon. The predominance of potassium feldspar in this wall rock, as opposed to plagioclase-feldspar in Holocene sediments, and the absence of iron-magnesium minerals are major differences between the mineral suites of the wall rock and unconsolidated sediments. Lithic fragments were the only dark grains observed in the wall rock. The clay-sized matrix, predominantly illite and kaolinite, is similar in composition to the unconsolidated pre-Holocene(?) sediments. Fossils, of early Pliocene age, from the wall rock indicate that the canyon has formed since early-Pliocene time.

### Sediment Transport

Grain-Size Distributions:--A wide range of grain-size distributions occurs among samples from cores (Appendix I, Figures 8-18). The sandy sediments are unimodal and muds are bimodal or polymodal. Pettijohn (1957) discussed the occurrence and causes of polymodal distributions in coarse-grained sediments but concluded that present data are insufficient to determine which causes are of greatest importance. Revelle (1944) attributed bimodal distributions in pelagic marine sediments of the north Pacific to the presence of organic debris. In general, polymodal distributions are interpreted as indicating several sources for sediment components or sorting processes which selectively remove some sediment sizes. Folk and Ward (1957) have observed bimodal distributions which resulted from mixing well-sorted sands from high energy neritic environments with fine-grained sediments of low energy, outer-shelf environments. A similar explanation may apply to the bimodal sediments in Willapa Canyon. Polymodal distributions might also result from differential settling of suspended material if the sedimentary components were characterized by different sizes and densities.

Abrupt changes in modes often occur between samples taken above and below discontinuities, indicating different sediment sources for adjacent layers. Identical minor modes occur every few layers in cores 326-47 and 326-49 (Appendix I, Figures 14, 16) suggesting that some sediment component has been added and removed. Core 326-48 illustrates an extreme situation in which major modes fluctuate; in this instance the modes occur in the sand class and can be related to bottom transport as discussed below.

Size-distribution curves must be interpreted with caution. Mixing of sediments by benthic organisms may cause similar modes to occur above and below discontinuities or, when sediments of adjacent layers have different textures, such mixing may cause mottling. In core 326-28, mixing of a sand layer into an underlying, fine-grained layer gave it the appearance of coarsening upward. Variable concentrations of organic skeletal debris might also cause the position of modes to fluctuate, particularly in size classes determined by pipette analysis, which measures particle density as well as grain size. When large percentages occur in several modes they probably represent several sediment-types which were first sorted in environments of different energy, and then mixed and deposited in their present environment, or a sediment that has been differentially sorted according to the settling velocities of its components.

Size-grading was observed in several cores, but is most pronounced in the coarse-grained layers of core 326-48 (Appendix I, Figure 15). Sand layers at 90, 180, and 190 centimeters are coarse-grained near the base, contain concentrations of heavy minerals, shell fragments, and pyrite-filled foraminifera. The upper limit of these layers is impossible to define and some may grade into pelagic sediments. The layer between 160-180 centimeters constitutes a single graded layer (Figure 15). Sand at the base of the layer grades upward into fine-grained sediment rich in diatoms, radiolaria, mica, and algal debris. The high organic-carbon content of the sample reflects this enrichment. Grading is also illustrated by a shift in the major modes of the size frequency curves for the interval. A similar example of grading is evident in the bed between 45 and 90 centimeters. The sample from 62 centimeters shows an increase in organic-carbon but, despite the similarity in texture, the increase is less than for the sample at 160 centimeters which marks the top of a layer.

Displaced Fauna:--Table 7 shows that, on the average, about 5 per cent of the individuals and 4-5 per cent of the species of foraminifera in surface samples from Willapa Canyon have been transported down slope. The greatest displacement occurs in cores of sandy sediments from the canyon axis. Core 326-48 (Table 8) shows a normal foraminiferal assemblage for that depth but the fauna below the surface of the core show a high percentage of displaced species. Little displacement of foraminifera is evident in core 326-36 or in surface samples from stations 326-47 and 326-49.

Fewer displaced foraminifera in sediment from the canyon walls suggest that it is moved less frequently and for shorter distances than sediment in axial regions. The absence of sandy lenses in sediments from the canyon walls indicates that little coarse material is being supplied into these regions. The low numbers of foraminifera in sediments throughout the canyon reflect the high rate of pelagic deposition.

Turbidity Currents:--Sands, interbedded with fine-grained sediments from the lower canyon, have the same heavy-mineral composition as shelf sands (Table 4) and contain shallow-water foraminifera (Table 8). The thin-bedded, rhythmic character of the sediments in many cores and the ubiquitous occurrence of ash and glauconite within the canyon indicate that the accumulation of sediment does not result from particle-by-particle deposition but probably was deposited from turbidity flows.

The presence of sands along canyon axes, presumed to mark routes followed by turbidity flows, has been noted by Emery (1960) and Emery and Hulsemann (1963). The same relationship in Willapa Canyon can be illustrated by considering cores 326-47, 326-48, 326-49, and 326-50 (Appendix I, Figures 14-17; Figure 2). Cores 326-47 and 326-49 (taken south and north of the canyon axis) consist of green mud, have few distinct discontinuities, and display fairly uniform distributions of grain-size, carbonate-carbon and organic-carbon. Cores 326-48 and 326-50 (from the canyon axis) consist of accumulations of graded layers separated by marked discontinuities and contain large percentages of sand. Further examples relating coarse-textured sediment to axial regions can be found by comparing Appendix I and Table 1 with the sample locations in Figure 2.

Some cores recovered from Cascadia Basin have sand layers about 1 meter thick and contain shallow water foraminifera (B. J. Enbysk, personal communication). The occurrence of thick sand layers in basin sediments, in contrast to the thin layers of graded sand in cores from the lower canyon, suggests that turbidity flows terminate west of Willapa Canyon, depositing little sediment within the canyon. Recovery of pre-Holocene(?) sediments in cores from the lower canyon also indicates that Holocene sediments are thin and that Willapa Canyon is essentially by-passed by sediment.

The topography of Cascadia Basin indicates that it has received great amounts of sediment. The basin is an elongate north-south depression, bounded on the east by the continental terrace and on the west by the seamount chain at 130-132 degrees west longitude. West of Willapa Canyon the basin reaches depths of 1300-1400 fathoms (2380-2560 meters). West of the seamount chain the seafloor drops abruptly to abyssal depths greater than 1700 fathoms (3100 meters). The broad, featureless plain of the basin floor, which slopes gently southward (McManus, 1964), suggests it has been filled with a thickness of sediment which could only have been derived from adjacent continental areas and transported across the continental terrace. Submarine canyons, such as Willapa Canyon, may act as conduits for this transport.

### Depositional Rates

The average depositional rate,  $50 \text{ mg cm}^{-2}\text{yr}^{-1}$ , obtained for core 326-36, is considered representative of pelagic sedimentation in the upper canyon area. Rates for the upper and lower portions of the core are nearly equal, indicating that sedimentation has been nearly constant during the last 6000 years. The rate of  $50 \text{ mg cm}^{-2}\text{yr}^{-1}$  is similar to the values given by Emery (1960, p. 254) for the continental borderland off southern California and is nearly the same as rates for Santa Cruz Basin ( $32.0 \text{ mg cm}^{-2}\text{yr}^{-1}$ ) and San Pedro Basin ( $35.2\text{-}52.9 \text{ mg cm}^{-2}\text{yr}^{-1}$ ).

The average sedimentation rate was used to obtain a surface sediment age of about 1477 years B.P., which compares with surface ages obtained for other samples off the Washington coast (D. A. McManus, personal communication). Average surface ages of 2400 years B. P. and 2900 years B.P. were obtained for six samples off southern California and for eight cores from the Atlantic (Emery, 1960). Emery (1960) has discussed possible causes of the great radiocarbon ages of surface sediments in basins off southern California, but concludes that our present knowledge is insufficient to explain the phenomenon. Likewise, although some significance is suspected, no explanation can be offered for the relatively young surface ages off the Washington coast.

Willapa Ash:--A depositional rate of  $50 \text{ mg cm}^{-2}\text{yr}^{-1}$  applied to the 240 centimeters of sediment overlying the ash layer in core 326-36 indicates that it was deposited about 5700 years B. P. The thickness of the layer (4 centimeters) and its distance from the nearest possible sources suggests that the ash was derived from a major volcanic eruption.

Ash deposits are common in many areas of western Washington. Of the five largest volcanoes of Washington, all except Mount Adams are reported to have ejected ash in Recent times (Rigg and Gould, 1957). Glacier Peak, whose activity culminated in a great eruption about 6700 years B. P., spread ash over an area of about  $5 \times 10^5$  square kilometers (Rigg and Gould, 1957). Mazama (Crater Lake) ash is abundant north and east of Crater Lake, Oregon, and is recognized on the Columbia Plateau of eastern Washington. The age of the Mazama ash is essentially the same as that of Glacier Peak, about 6500 (Libby, 1952) or 6600 (Powers and Wilcox, 1964) years B.P.

Although the ash layer from Willapa Canyon records a major volcanic event, it is difficult to assign it a source because: (1) the petrographic similarity of ash deposits from the Cascade volcanoes (Rigg and Gould, 1957) generally prohibits positive identification of ash from different areas by petrographic criteria; (2) ash deposits of Holocene age have not previously been reported west of the vicinity of Olympia, Washington (Rigg and Gould, 1957); and (3) the radiocarbon age of the ash from core 326-36 is younger than that generally accepted for Glacier Peak and Mazama ash.

Comparative study of Glacier Peak (Rigg and Gould, 1957) ash from Lake Washington, Seattle and from near the town of Twisp in northcentral

Washington with the Willapa ash was inconclusive. The sample from Willapa Canyon is somewhat devitrified and chloritized, preventing comparison of crystalline mineral components. The indices of refraction of the three samples are very nearly the same, approximately 1.505; an average also obtained by Rigg and Gould (1957) for fourteen Glacier Peak ash samples from peat bogs.

New Petrographic and chemical data (Powers and Wilcox, 1964) indicate that the Mount Mazama eruption was the source of most ash which has been called Glacier Peak (Rigg and Gould, 1957) and some of the ash called Galata (near Galata, Montana). Glacier Peak is believed to be the source of an older ash deposit of possible late glacial or early postglacial age. Both Glacier Peak and Mazama ash were widely deposited. Powers and Wilcox (1964) report two localities in eastern Washington and one in Idaho where Mazama ash stratigraphically overlies Glacier Peak ash. The Glacier Peak ash has indices of refraction in the range of 1.495 to 1.500 with values as low as 1.486 rarely encountered; Mazama ash has a slightly higher range with dominant values between 1.500 and 1.510 (Wilcox and Powers, 1963; Powers and Wilcox, 1964). Thus, on the basis of refractive index, the Willapa ash most closely resembles the Mazama ash of Powers and Wilcox.

The depositional rate computed for core 326-36 would generally be considered a minimum because it rests on the assumption that neither diastems nor erosional disconformities are present in the core. A greater depositional rate, however, would give an even younger age for the ash layer. If the ash was derived from the Glacier Peak (Rigg and Gould, 1957) or Mazama (Powers and Wilcox, 1964) eruption, an age younger than 5700 years B.P. is doubtful and the computed depositional rate is probably a maximum. Computation based on an age of 6600 years B.P. (Powers and Wilcox, 1964) for the ash gives a depositional rate of about  $44 \text{ mg cm}^{-2} \text{ yr}^{-1}$ , a value not significantly less than the rate obtained previously. Positive identification of the source of the Willapa ash would provide a check on the carbon-14 dates and depositional rates obtained in this study.

Ash layers similar to the one from Willapa Canyon have not been previously reported from the continental terrace off Washington. Perhaps a major portion of the ash layer has been transported downslope and mixed with sediments in deeper water. If the ash is not widely distributed, its significance as a stratigraphic marker is reduced and the chances of obtaining additional samples to substantiate data presented here are lessened. It should be noted however that, if it lies at a depth of 3 meters beneath the sediment surface, few cores of sufficient length to penetrate the layer have been taken on the slope.

The potential value of the ash as a stratigraphic marker is increased by its occurrence in Holocene sediments of Washington and adjacent areas. The extent of its usefulness in correlating marine and terrestrial post-glacial events must await further proof of its distribution in marine sediments.

## CONCLUSIONS

1. Well sorted sands are common on the shelf near the head of Willapa Canyon and green pelagic muds are the dominant sediment-type within the canyon. Sand occurs within the canyon but is confined to axial areas.
2. Illite, Fe-chlorite, and kaolinite are the major clay minerals in the area studied. The clay-mineral suite in the average sediment contains about 20 per cent Fe-chlorite, 30 per cent kaolinite, 50 per cent illite.
3. The organic-carbon content of canyon sediments ranges from about 0.2-2.9 per cent and varies inversely with the grain size. The lowest concentrations of organic matter occur in sediments believed to be pre-Holocene. The average carbon-nitrogen ratio, 9.0, indicates that marine organisms are the predominant source of this material.
4. The carbonate-carbon content of most sediments ranges between 0.05 and 1.5 per cent. Shelf sands are low in carbonate while sand layers on the slope, containing shell fragments and micro organisms, have higher values. The highest carbonate concentrations were measured in sediments of suspected pre-Holocene age.
5. The Columbia River is apparently the principle source of sand and mud deposited within the canyon. Contributions from the canyon walls and from wind-born sediment are believed to be negligible.
6. Turbidity flows, originating on the upper slope and shelf, transport the major portion of their sediment load to Cascadia Basin west of the study area. Only minor thicknesses of sediment are deposited within the canyon.
7. The maximum rate of deposition on the upper slope near Willapa Canyon is about  $50 \text{ mg cm}^{-2}\text{yr}^{-1}$  and has been nearly constant during the last 6000 years.
8. The total accumulated thickness of Holocene sediment within most of the canyon is only several meters. Areas of low relief may accumulate slightly greater thicknesses.
9. Bed rock, dredged from the canyon walls, contains fossils which suggest the canyon has been formed since early-Pliocene time.

## REFERENCES

- American Society for Testing and Materials. 1962. Index to the X-ray powder data file. Am. Soc. Testing Mater. Spec. Tech. Publ. 48-L, 368 p.
- Anderson, N. K. 1962. Recent sediments of Deep Inlet, Alaska. M.S. Thesis. Univ. Washington, Seattle, Washington. 152 p.
- Bader, R. G. 1955. Carbon and nitrogen relations in surface and sub-surface marine sediments. *Geochim. Cosmochim. Acta*, 7:205-211.
- Ballard, R. L. 1964. Distribution of beach sediment near the mouth of the Columbia River. Univ. Washington Dept. Oceanog. Tech. Rept. 98, 81 p.
- Brown, G. (ed.). 1961. The X-ray identification and crystal structures of clay minerals. Mineralogical Society (Clay Minerals Group), London. 544 p.
- Burst, J. F. 1958. Glauconite pellets: their material nature and applications to stratigraphic interpretations. *Bull. Am. Assoc. Petrol. Geol.*, 42:310-327.
- Cohee, G. V. 1938. Sediments of the submarine canyons off the California coast. *J. Sediment. Petrol.*, 8:19-33.
- Creager, J. S., D. A. McManus, and E. E. Collias. 1962. Electronic data processing in sedimentary size analysis. *J. Sediment. Petrol.*, 32:833-839.
- Creager, J. S., and R. W. Sternberg. 1963. Comparative evaluation of three techniques of pipette analysis. *J. Sediment. Petrol.*, 33:462-466.
- Emery, K. O. 1960. The sea off southern California: a modern habitat of petroleum. Wiley, New York. 366 p.
- Emery, K. O., and J. Hulsemann. 1963. Submarine canyons of southern California. *Allen Hancock Expeditions*, 27(1):1-80.
- Fessenden, F. W. 1959. Removal of heavy liquid separates from glass centrifuge tubes. *J. Sediment. Petrol.*, 29:621.
- Folk, R. L., and W. C. Ward. 1957. Brazos river bar: a study in the significance of grain size parameters. *J. Sediment. Petrol.*, 27:3-26.
- Geological Society of America. 1951. Rock Color Chart. Geol. Soc. Am., New York.

- Gorsline, D. S., and K. O. Emery. 1959. Turbidity-current deposits in San Pedro and Santa Monica basins off southern California. *Bull. Geol. Soc. Am.*, 70:270-290.
- Griffin, J. J., and E. D. Goldberg. 1963. Clay mineral distributions in the Pacific Ocean, p. 728-741. In M. N. Hill, (ed.), *The Sea*. Interscience, New York. Vol. III.
- Grim, R. E. 1951. The depositional environment of red and green shales. *J. Sediment. Petrol.*, 21:226-232.
- Grim, R. E. 1953. *Clay mineralogy*. McGraw, New York. 384 p.
- Gripenberg, S. 1934. A study of the sediments of the North Baltic and adjoining seas. *Fennia*, 60:130-176.
- Gucluer, S. M. 1962. Recent sediments in Saanich Inlet, British Columbia. M.S. Thesis. Univ. Washington, Seattle, Washington. 119 p.
- Hedgpeth, J. W. 1957. Obtaining ecological data in the sea, p. 53-86. In J. W. Hedgpeth, (ed.), *Treatise on marine ecology and paleoecology*. *Geol. Soc. Am.*, New York. Vol. I.
- Inman, D. L. 1952. Measures for describing size of sediments. *J. Sediment. Petrol.*, 22:125-145.
- Jackson, M. L. 1958. *Soil chemical analysis*. Prentice-Hall, Englewood Cliffs, New Jersey. 498 p.
- Keller, W. D. 1953. Illite and montmorillonite in green sedimentary rocks. *J. Sediment. Petrol.*, 23:3-9.
- Koczy, F. F. 1963. Age determination in sediments by natural radioactivity, p. 816-831. In M. N. Hill, (ed.), *The Sea*. Interscience, New York. Vol. III.
- Krumbein, W. C., and F. J. Pettijohn. 1938. *Manual of sedimentary petrography*. 2nd ed. Appleton-Century, New York. 535 p.
- Kullenberg, B. 1947. The piston core sampler. *Sv. Hydr.-Biol. Komm. skr. Ser. 3*, 2:1-46.
- Libby, W. F. 1952. *Radiocarbon dating*. Univ. of Chicago Press, Chicago. 124 p.
- McManus, D. A. 1964. Major bathymetric features near the coast of Oregon, Washington, and Vancouver Island. *Northwest Sci.*, 38:65-82.
- Pettijohn, F. J. 1957. *Sedimentary rocks*. 2nd ed. Harper, New York. 718 p.

- Powers, H. A., and R. E. Wilcox. 1964. Volcanic ash from Mount Mazama (Crater Lake) and from Glacier Peak. *Science*, 144: 1334-1336.
- Revelle, R. 1944. Marine bottom samples collected in the Pacific Ocean by the Carnegie on its seventh cruise. Carnegie Inst. Wash. Publ. 556(1944). 80 p.
- Rigg, G. B., and H. R. Gould. 1957. Age of Glacier Peak eruption and chronology of post glacial peat deposits in Washington and surrounding areas. *Am. J. Sci.*, 255:341-363.
- Scholl, D. W. 1963. Sedimentation in modern coastal swamps, southwestern Florida. *Bull. Am. Assoc. Petrol. Geol.*, 47:1581-1603.
- Shepard, F. P. 1939. Continental shelf sediments, p. 219-229. *In* P.D. Trask (ed.), *Recent marine sediments*. Am. Assoc. Petrol. Geol., Tulsa.
- Shepard, F. P. 1954. Nomenclature based on sand-silt-clay ratios. *J. Sediment. Petrol.*, 24:151-158.
- Shepard, F. P. 1963a. *Submarine geology*. 2nd ed. Harper, New York. 557 p.
- Shepard, F. P. 1963b. Submarine canyons, p. 480-506. *In* M. N. Hill, (ed.), *The Sea*. Interscience, New York. Vol. III.
- Shepard, F. P., and C. N. Beard. 1938. Submarine canyons: distribution and longitudinal profiles. *Geograph. Rev.*, 28:439-451.
- Shepard, F. P., and K. O. Emery. 1941. Submarine geology off the California coast: canyons and tectonic interpretations. *Geol. Soc. Am. Spec. Paper* 31. 171 p.
- Sternberg, R. W., and J. S. Creager. 1961. Comparative efficiencies of size analysis by hydrometer and pipette methods. *J. Sediment. Petrol.*, 31:96-100.
- Stetson, H. C. 1936. Geology and paleontology of the Georges Bank Canyons. *Bull. Geol. Soc. Am.*, 47:339-366.
- Sverdrup, H. U., M. V. Johnson, and R. H. Fleming. 1942. *The oceans, their physics, chemistry, and biology*. Prentice-Hall, Englewood Cliffs, New Jersey. 1087 p.
- Trask, P. D. 1932. Origin and environment of source sediments of petroleum. Gulf Publishing Co., Houston. 323 p.
- Trask, P. D. 1939. Organic content of recent marine sediments, p. 428-453. *In* P. D. Trask, (ed.), *Recent marine sediments*. Am. Assoc. Petrol. Geol., Tulsa.

- Van Veen, J. 1936. Onderzoekingen in de Hoofden. Landsdrukkerij, The Hague. 252 p.
- Von Arx, W. S. 1962. An introduction to physical oceanography. Addison-Wesley, Reading, Massachusetts. 422 p.
- Waksman, S. A. 1931. On the distribution of organic matter on the sea bottom and the chemical nature and origin of marine humus. Woods Hole Oceanog. Inst. Contrib., 5:125-145.
- Weaver, C. E. 1958. Geologic interpretation of argillaceous sediments. Part I. Origin and significance of clay minerals in sedimentary rocks. Bull. Am. Assoc. Petrol. Geol., 42:254-271.
- Wilcox, R. E., and H. A. Powers. 1963. Petrographic characteristics of recent pumice from volcanoes in the Cascade Range. Abstr. 59th Ann. Meeting Geol. Soc. Am., p. 64.

## APPENDIX I

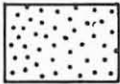
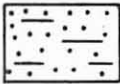
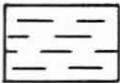
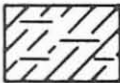
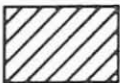

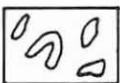
CORE DATA FROM BROWN BEAR CRUISE 326Explanation of Figures 8-18

Figures 8-18 show the variation of sediment parameters with depth in cores from Brown Bear cruise 326. The sand-silt-clay percentage bars in column two intercept an interval of the lithology column approximately equivalent to the sampling interval in the cores. The scales used for median diameter ( $Md_{\phi}$ ), total-carbon, and organic-carbon are constant but the carbonate-carbon scale varies among the figures. Carbon values are expressed as per cent, by weight, of dry sediment.

Size-frequency distribution curves are shown for each sample and indicate the percentage weight of sediment occurring in each phi interval. The total area under each curve equals 100 per cent of the sample weight. The notation "trigger core" refers to the short gravity corer used to trigger the piston corer.

The lithology shown is generalized and is that which would be applied in the field. Color designations are from the Rock Color Chart (Geologic Society of America, 1951) and apply to the wet sediment. Discontinuities are based largely on evidence from X-radiographs. The lithologic symbols used are defined below. Data for surface samples are shown in figure 19.

## LITHOLOGIC SYMBOLS

	SAND		SILTY SAND
	SILT		SILTY CLAY
	CLAY		SIZE GRADING (from sand to clay)
	MOTTLING		



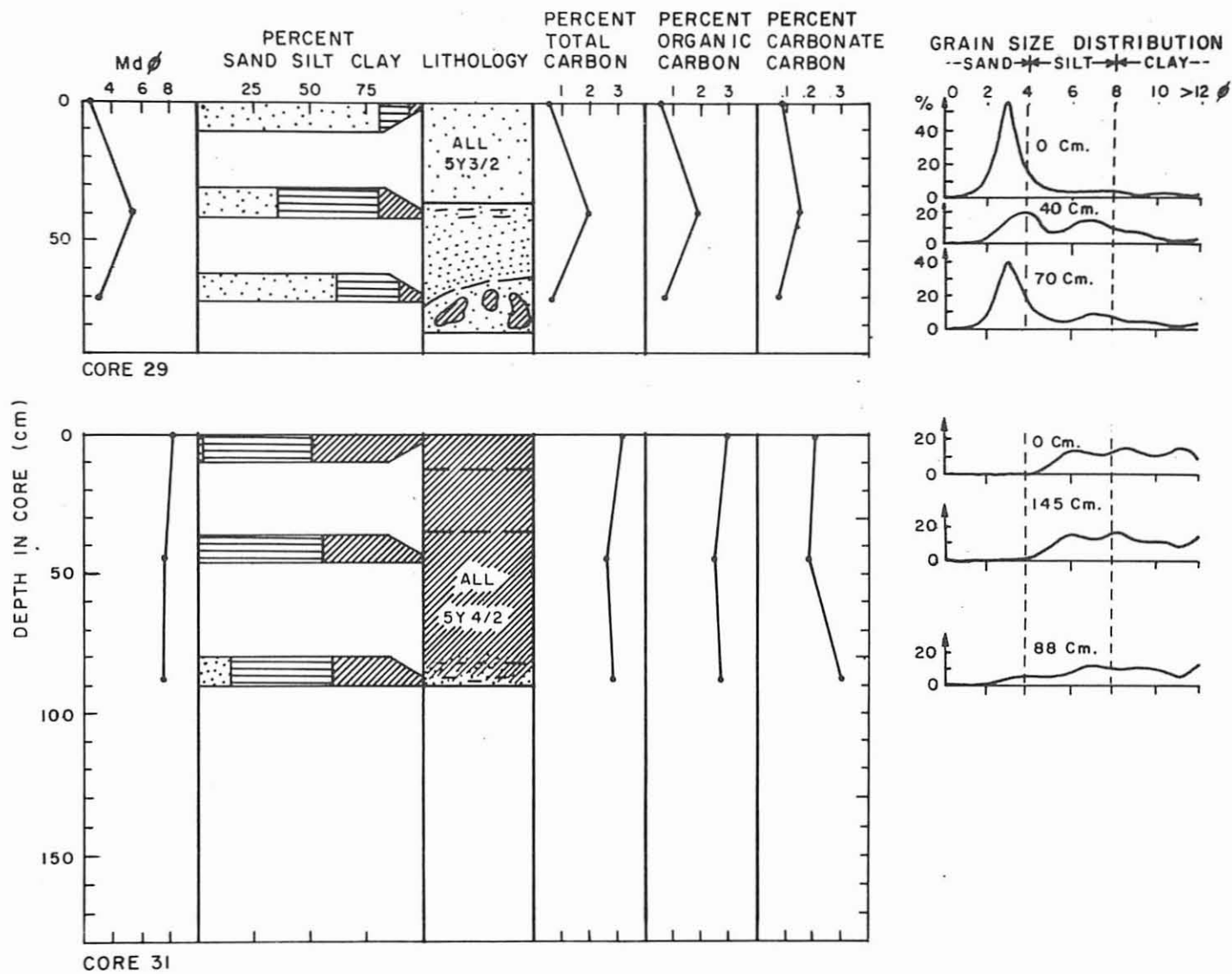
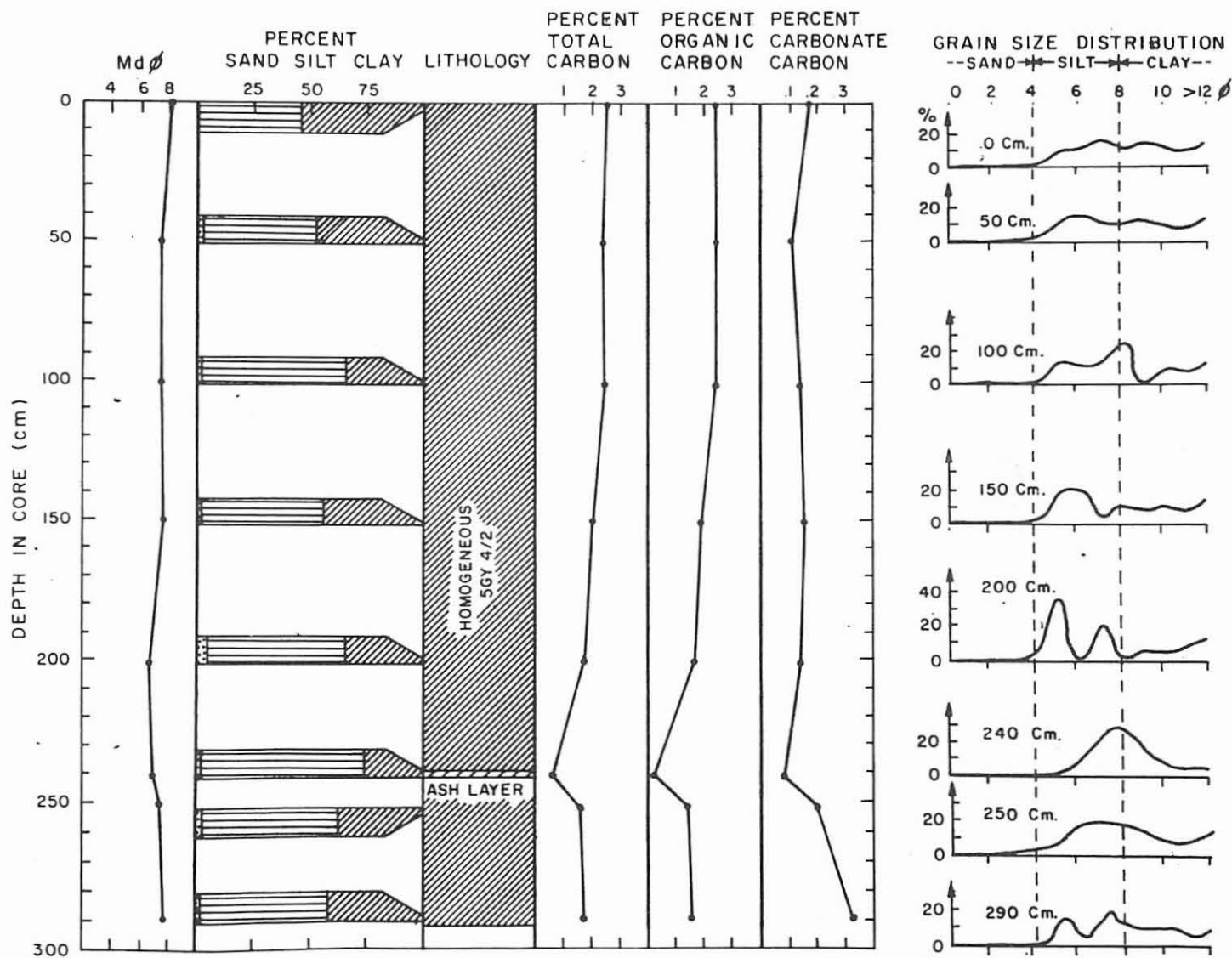


Fig. 9. Sediment parameters versus depth in cores.



CORE 36.

Fig. 10. Sediment parameters versus depth in cores.

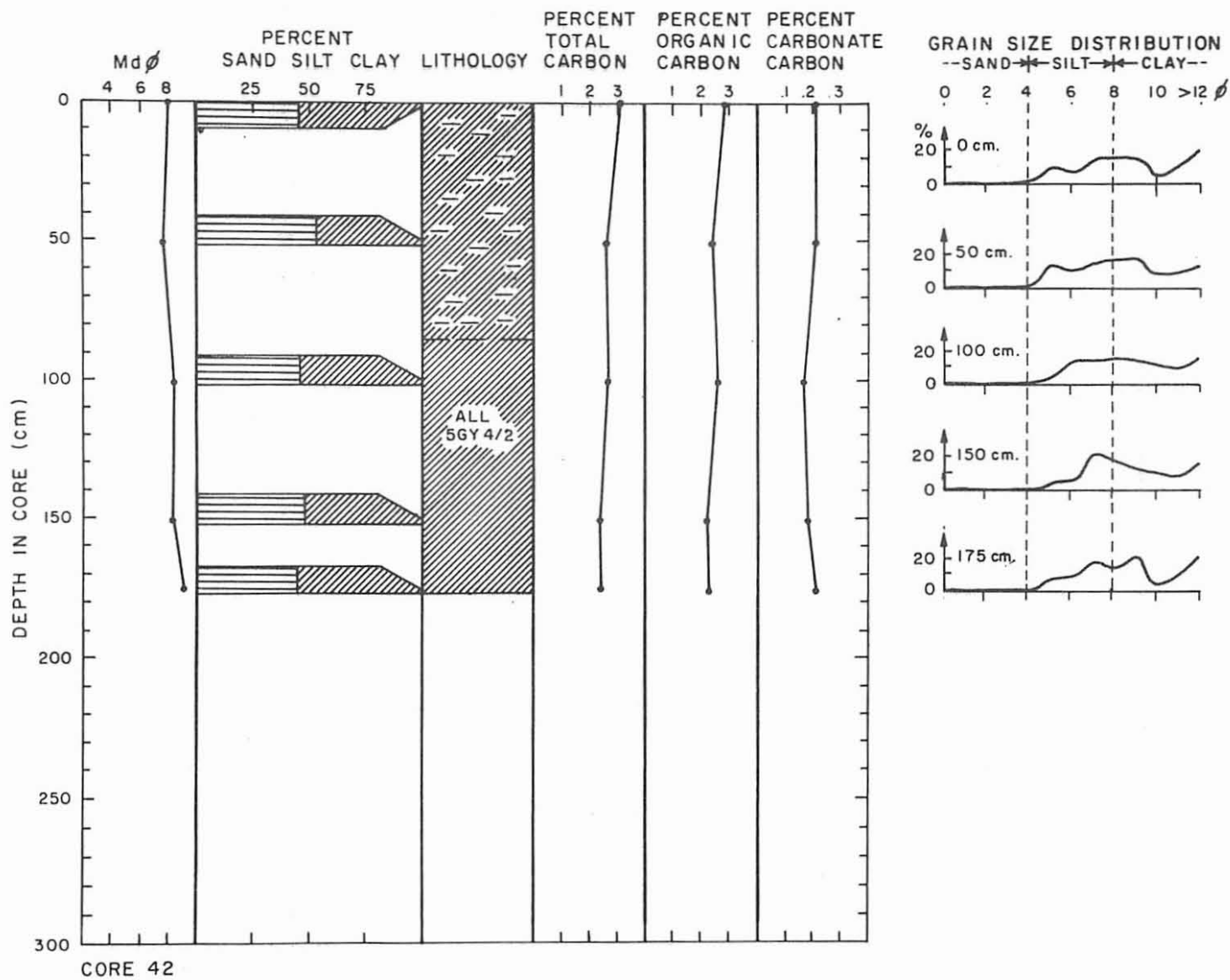


Fig. 11. Sediment parameters versus depth in cores.

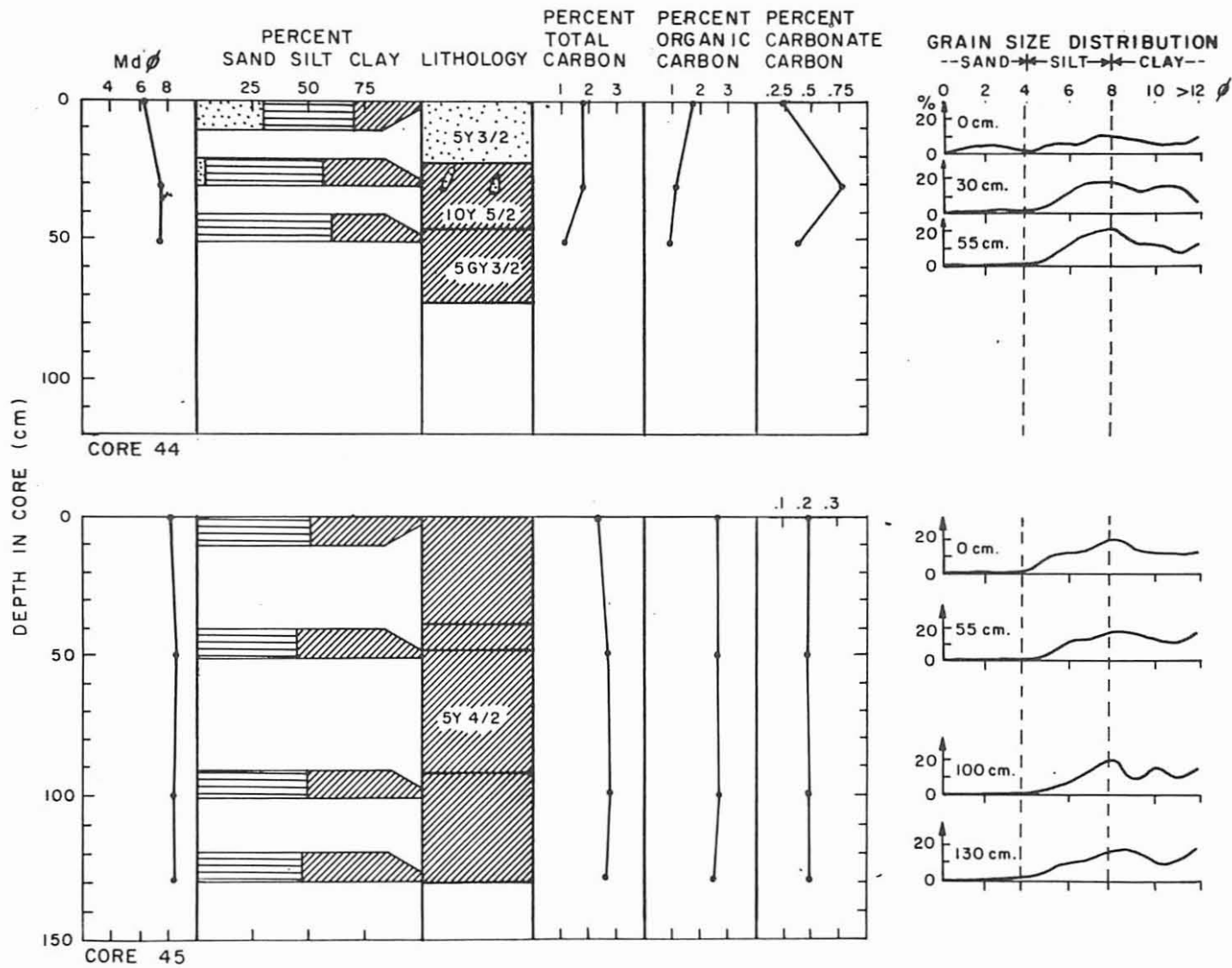


Fig. 12. Sediment parameters versus depth in cores.

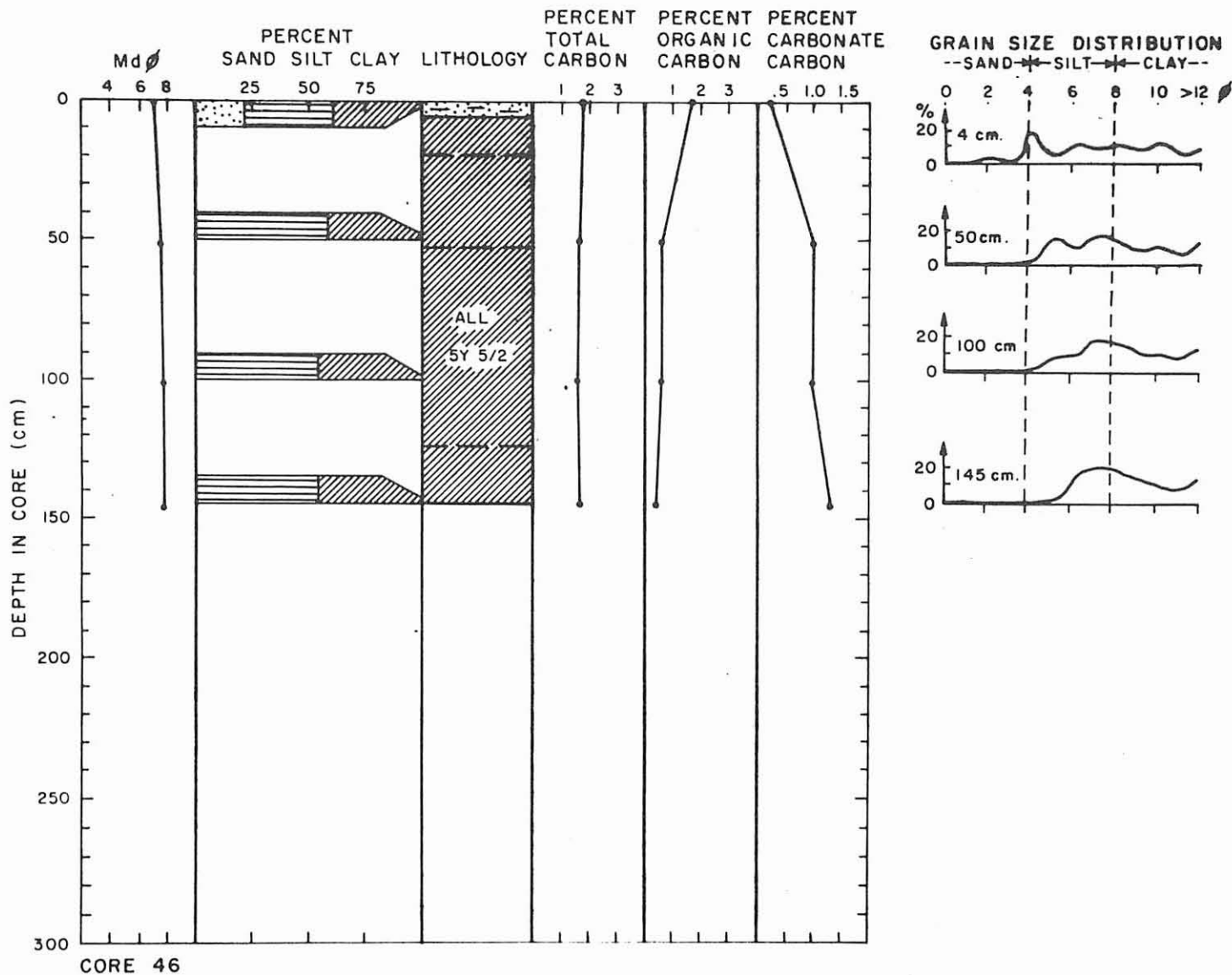


Fig. 13. Sediment parameters versus depth in cores.

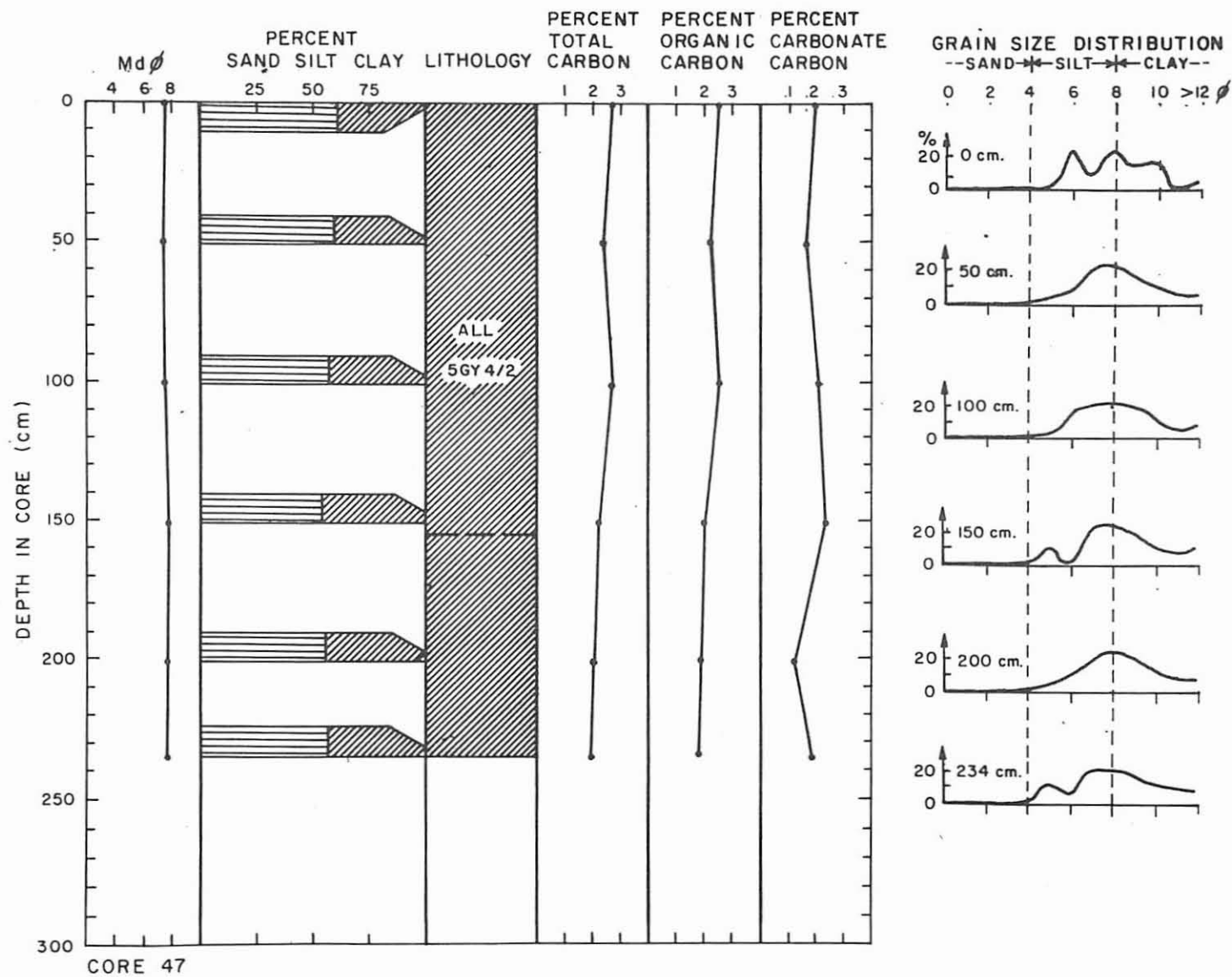


Fig. 14. Sediment parameters versus depth in cores.

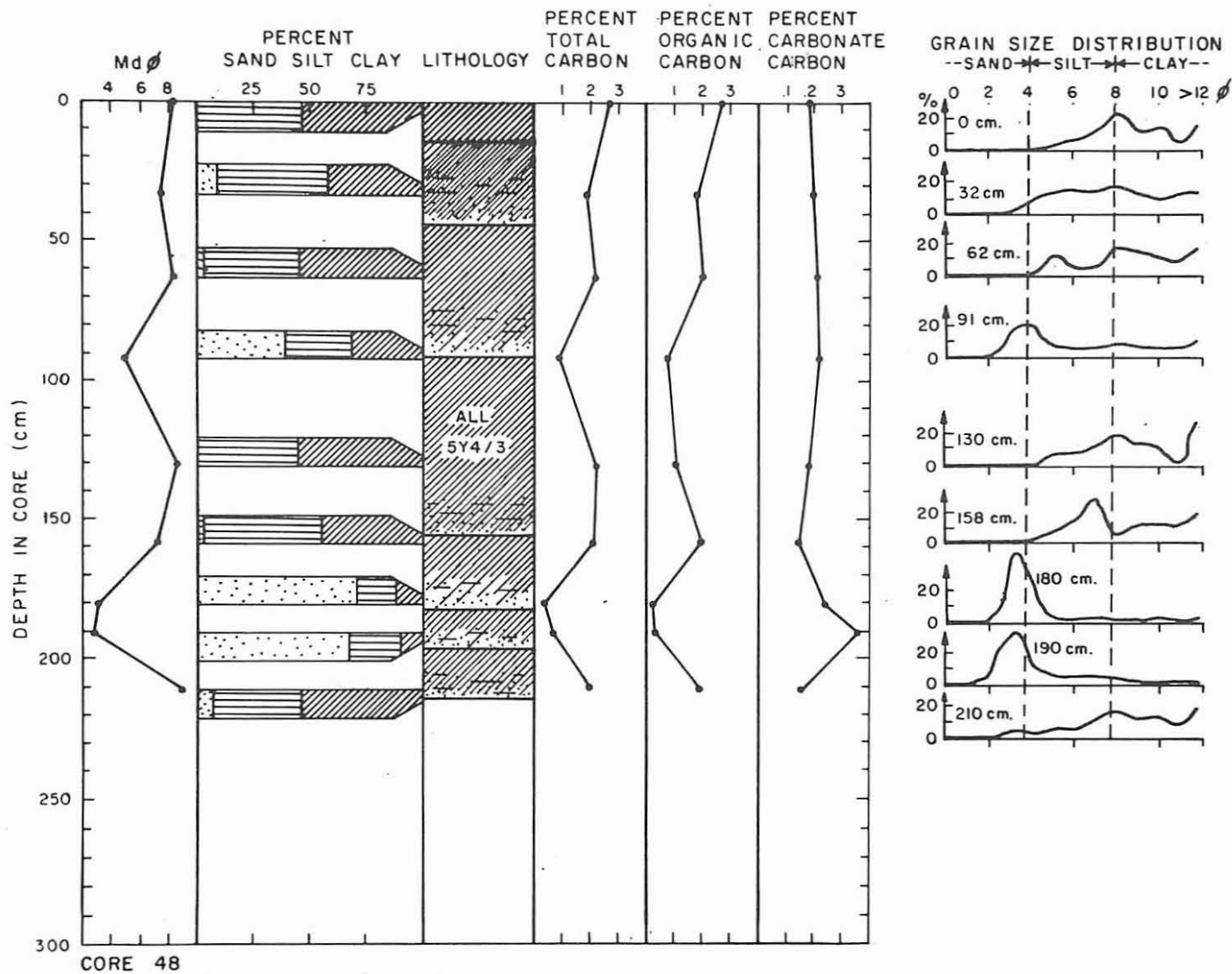


Fig. 15. Sediment parameters versus depth in cores.

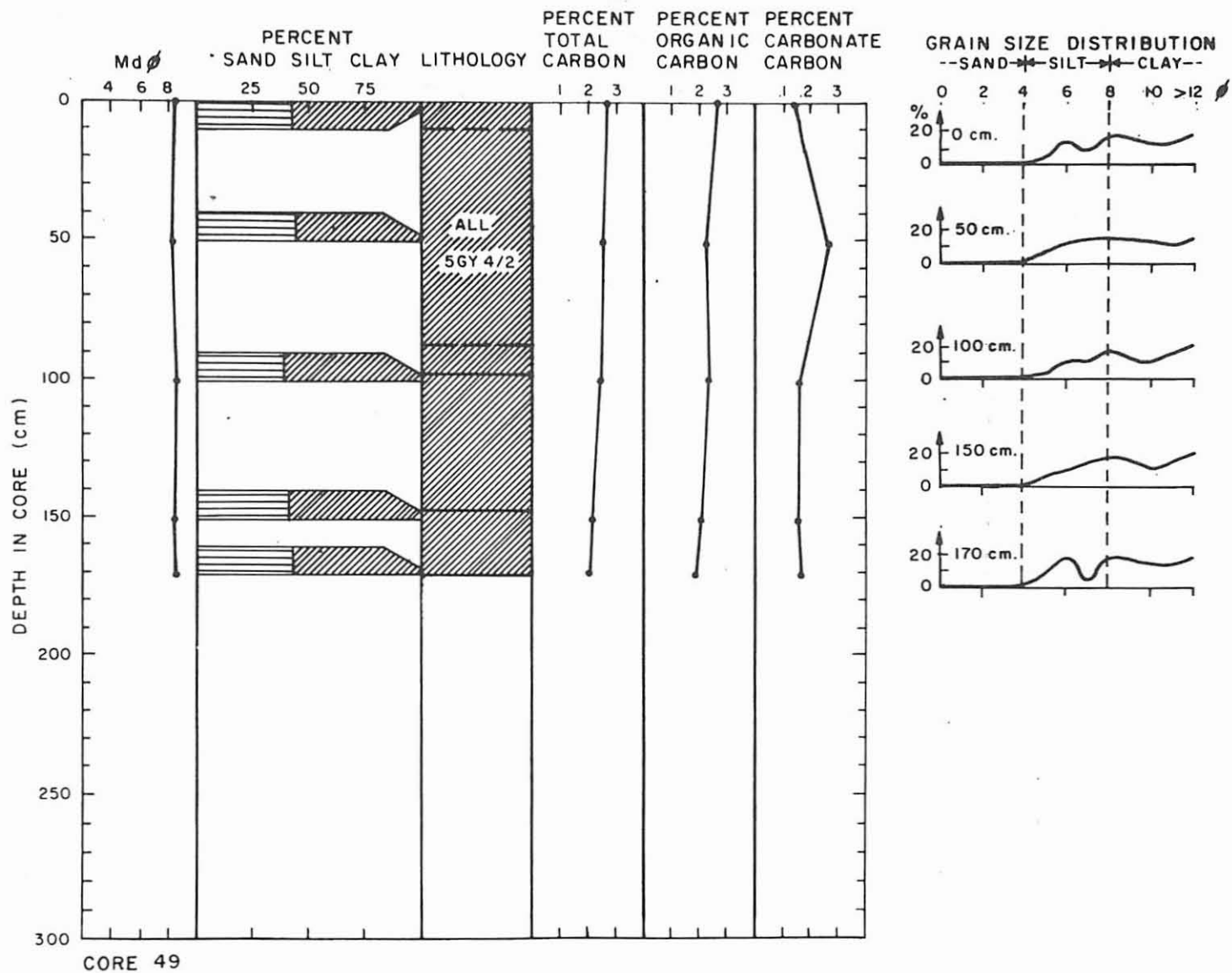


Fig. 16. Sediment parameters versus depth in cores.

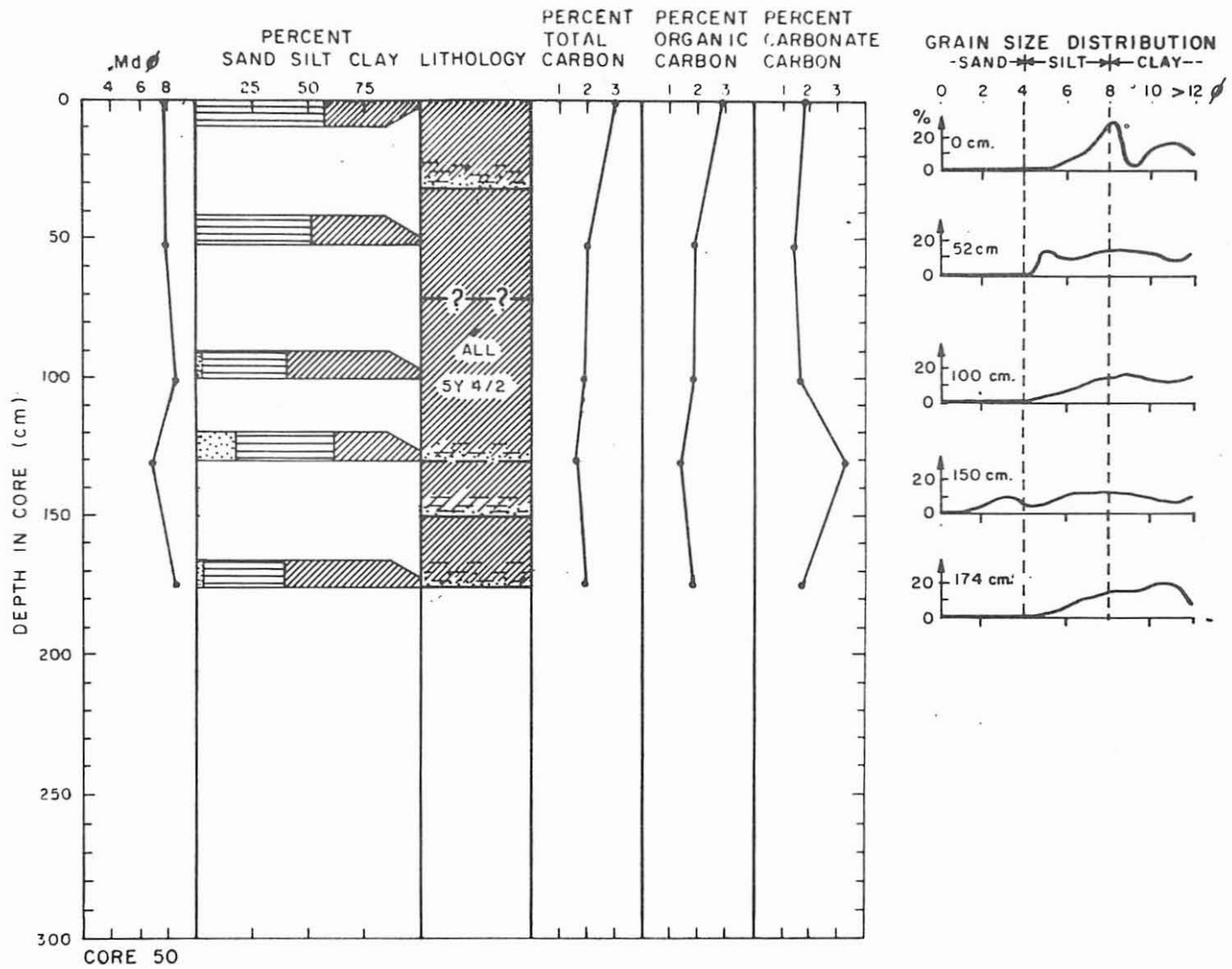


Fig. 17. Sediment parameters versus depth in cores.

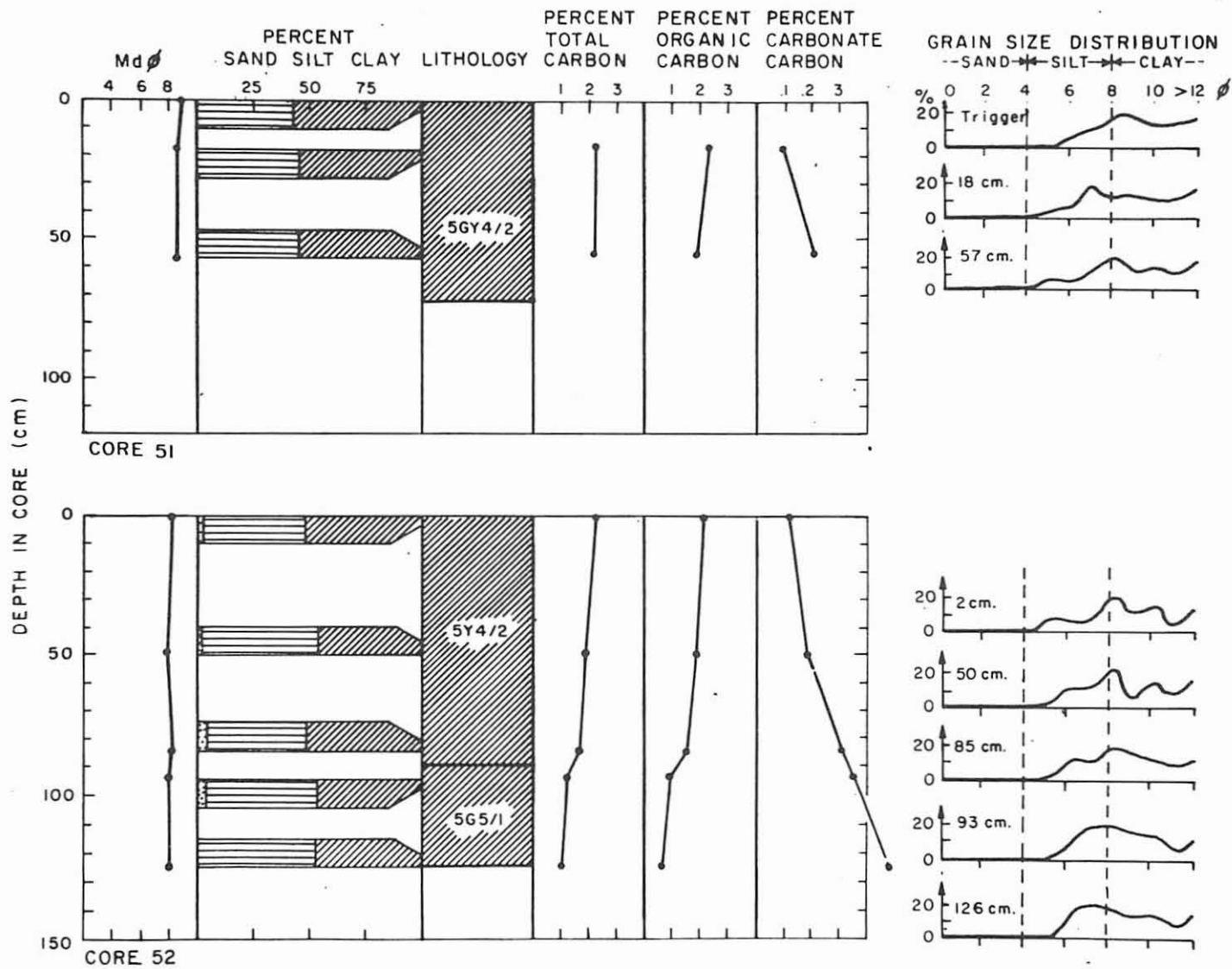


Fig. 18. Sediment parameters versus depth in cores.

STATION	Md $\phi$	PERCENT			PERCENT TOTAL CARBON	PERCENT ORGANIC CARBON	PERCENT CARBONATE CARBON
		SAND	SILT	CLAY			
28	6.8	12.7	51.1	36.2	0.80	0.72	0.08
29	2.6	82.5	10.8	6.7	2.29	0.29	2.00
39	1.8	83.2	9.7	7.1	0.74	0.69	0.05
37	7.9	1.0	50.1	48.9	3.02	2.84	0.18

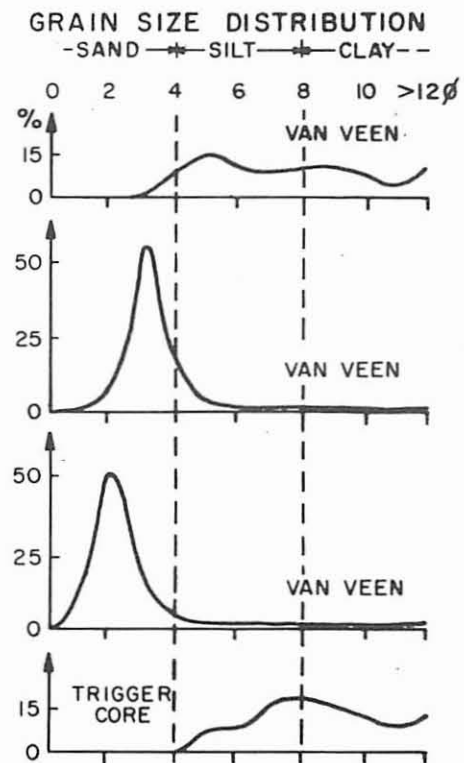


Fig. 19. Sediment parameters of surface samples.

## APPENDIX II

## ANALYTICAL PROCEDURES

Preliminary Treatment and Sampling

Cores from Brown Bear cruise 326 were cut horizontally and one half was sealed in a plastic D-tube and retained for reference in refrigerated storage. Colors, textures, and structures (Appendix I) were recorded and X-radiographs obtained of each wet core prior to removal of samples for size and chemical analyses.

Samples for analyses were taken from each distinct sediment layer within the wet core, or at 50-centimeter intervals if the sediment appeared homogenous. In most cases samples were taken above and below marked discontinuities.

Size Analysis

Approximately 10 grams (dry weight) of each sample was washed with distilled water for 20 minutes and decanted. It was assumed that sediment lost with the supernatant liquid was negligible (Creager and Sternberg, 1963). The washed sample was dispersed with Marasperse (sodium lignosulfonate: 0.1 grams/liter) in a malt mixer for 15 minutes and sieved through a 4-phi<sup>4</sup> (62-microns) screen into a one-liter cylinder. Sediment retained on the sieve was dried and shaken for 10 minutes in 3-inch Tyler Standard Screens, arranged in a single phi-unit progression from 0 to 4 phi, in an automatic shaker.

Pipette analysis was made of the clay- and silt-sized sediment in the cylinders (Krumbein and Pettijohn, 1938; Sediment Analysis Laboratory, University of Washington, unpublished). Twenty-milliliter aliquots were taken at selected times, dried (60 degrees Celcius), and weighed to the nearest milligram.

Sediment weights of the phi size-classes for both sieve and pipette fractions were processed by a computer program (Creager et. al., 1962) to obtain fractional and cumulative percentage values of size classes, sand-silt-clay relationships, and the statistical parameters of Trask (1932), Inman (1952), and Folk and Ward (1957).

Multiple analyses of sediments similar to those from Willapa Canyon indicate that the reproducibility of cumulative data from pipette analysis is about  $\pm 1.0$  phi units at the 50th percentile (Sternberg and Creager, 1961). Thus, the mean diameter of a fine-grained sediment may be reproduced, with 95 per cent confidence, only within  $\pm 1.0$  phi units. Differences in sediment concentrations and water temperatures in the settling cylinders appear to be the major causes of variable results among samples of the same or similar size composition.

---

<sup>4</sup> Grain size in phi values is defined as the negative log to the base two of the grain diameter in millimeters ( $\text{phi} = \log_2 \text{size in millimeters}$ ).

## Chemical Analysis

Concentrations of total-carbon and carbonate-carbon were obtained by gasometric analysis using a LECO (Laboratory Equipment Company) induction furnace (model 521) and carbon determinator (model 572-200). About 0.5 gram of finely ground sample was placed in a ceramic crucible (with small amounts of iron accelerator and tin catalyst) and ignited in the furnace in an oxygen atmosphere. The exact temperature of ignition is not known but it was presumed to be about 2000 degrees Celcius. The combustion products and excess oxygen were collected over sulfuric acid, and the amount of  $\text{CO}_2$  produced was determined by passing the gas from the burette into a KOH solution which absorbed the  $\text{CO}_2$ . The remaining gases were brought back into the burette and the removed  $\text{CO}_2$  was measured by difference. The per cent carbon per gram, read directly from the burette, was corrected for temperature and ambient pressure.

The reproducibility and accuracy of the system was determined by analysis of ten 1.0-gram samples of NBS carbon steel (51-b) containing 1.2 per cent carbon. Reproducibility was  $\pm 0.03$  per cent, giving an accuracy of 2.5 per cent.

Carbonate-carbon analysis was similar to that for total-carbon except that  $\text{CO}_2$  was evolved by acid treatment. About 2 grams of finely ground, washed sediment were reacted with 10 milliliters of phosphoric acid in a flask which was gently heated to boiling. The evolved gases were drawn through a condensing column into the carbon determinator and the  $\text{CO}_2$  content measured as described above. Flushing of the system was achieved, after complete acid reaction, by admitting  $\text{CO}_2$ -free air into the flask. Analysis of laboratory-grade, chemically pure  $\text{CaCO}_3$  indicated that results were slightly high. The accuracy of the method was approximately 1 per cent.

Total-nitrogen values were measured for eight samples by the macro-Kjeldahl method (Jackson, 1958) in the Soil Chemistry Laboratory of the Forestry Department, University of Washington.

A mixture of 32 parts  $\text{CuSO}_4$  and 1000 parts  $\text{N}_2\text{SO}_4$ , a pellet of Se catalyst, and 35 milliliters of concentrated  $\text{H}_2\text{SO}_4$  were added to the 3-6 grams of sample and the solution boiled to clearness (about 3 hours). The solution was cooled, diluted with distilled water, and a zinc pellet and 125 milliliters of concentrated NaOH added. The solution was then distilled for 30 minutes into boric acid, titrated with standard  $\text{H}_2\text{SO}_4$ , and the equivalent of nitrogen computed.

## X-Ray Identification of Clay Minerals

Slides for X-ray diffraction of the clay-sized fraction of all samples were prepared during pipette analysis. An extra 9-phi aliquot was pipetted into a beaker containing a glass slide and several milliliters of bonding agent consisting of a dilute solution of water soluble glue. The samples were dried at 60 degrees Celcius.

Equipment consisted of a Norelco X-ray diffraction unit with a copper X-ray tube, a wide-range goniometer and Argon geiger-counter (62019), and an REAC Model H-580 rate-meter. Results were recorded on a strip-chart recorder at scale speed of one-half inch per minute. Samples were scanned through  $60^\circ (2\theta)$  at  $1^\circ (2\theta)$  per minute.

The d-spacings were determined by use of a template. The d-spacings were compared with those tabulated by the ASTM in the Index to the X-Ray Powder Data File (1962) for mineral identification.

An initial analysis was made with air dried sample. A second analysis of most samples was made after exposure to ethylene-glycol vapor in a vacuum desiccator (20-25 degrees Celcius), a treatment which expands the crystal lattice of montmorillonoids. Sedimented slides were also analyzed after acid and heat treatment (Brown, 1961). Treatment with 2N HCl (which destroys the iron lattice of Fe-chlorite) removed the 14 Angstrom and reduced the 7.1 and 3.5 Angstrom peaks on diffractograms (Figure 20; B and C, E and F). Subsequent heating at 550-600 degrees Celcius for one hour (which converts kaolinite to an amorphous state) caused removal of peaks at 7.1 and 3.5 Angstroms (Figure 20; C and D).

Mica-species with X-ray diffraction peaks at 5.0 and 10 Angstroms which were unaffected by ethylene-glycol, acid, and heat treatments were identified as illite (Brown, 1961). The presence of a 14 Angstrom peak which was removed (or greatly reduced) by acid treatment was considered evidence of the presence of Fe-chlorite (Weaver, 1958). Double or broad peaks near 3.5 Angstroms on diffractograms of untreated samples indicated the common occurrence of kaolinite and Fe-chlorite. Peaks remaining at 7.1 and 3.5 Angstroms after acid treatment were attributed to kaolinite.

Montmorillonoids in untreated samples give a broad, diffuse peak above 14 Angstroms which may be confused with mixed-layer clays. They are identified with certainty only after exposure to ethylene-glycol vapors which expand the (001) lattice to about 17 Angstroms. This treatment generally had no effect in the samples analyzed (Figure 20; A and B).

The presence of mixed-layer clays was indicated by a broad, diffuse peak (high background intensity) above 12 or 13 Angstroms (Figure 20; A, B, and E). Reduction of this plateau by acid treatment suggested that the mixed-layers contain large amounts of Fe-chlorite (Figure 20; E and F). Reduction after heat treatment indicated that the mixed-layers contained kaolinite (Figure 20; C and D). Broadening of the 10 Angstrom peak after heat treatment resulted from collapse of montmorillonite-type layers (Figure 20; D).

The presence of minerals composing 5-10 per cent of a sample can generally be determined by X-ray diffraction. Minerals with well developed, crystalline structures are detected with greatest reliability and members of mineral series or groups are identified with less certainty. Diffraction peaks with intensities twice that of the average background were used for mineral identification.

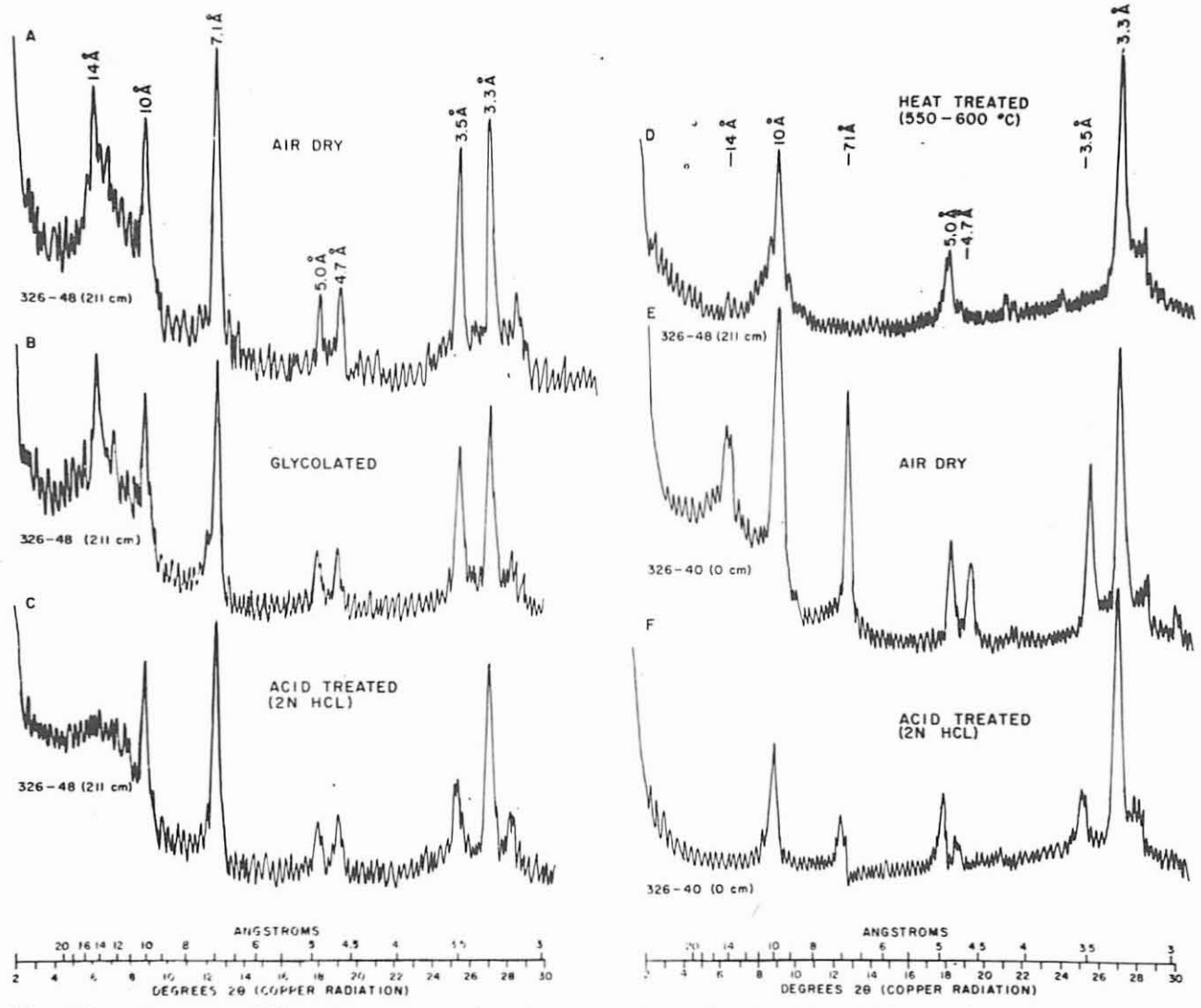


Fig 20. X-ray diffractograms showing results of glycol, acid, and heat treatments.

APPENDIX III  
STATISTICAL PARAMETERS

INMAN VALUES are statistical parameters calculated from cumulative-frequency curves according to Inman (1952).

The formulas used are:

MEDIAN DIAMETER = 50th percentile value

MEAN =  $\frac{16\text{th percentile} + 84\text{th percentile}}{2}$

DEVIATION =  $\frac{84\text{th percentile} - 16\text{th percentile}}{2}$

this latter gives a measure of sorting.

SKEWNESS =  $\frac{\text{MEAN} - \text{MEDIAN}}{\text{DEVIATION}}$

2nd SKEWNESS =  $\frac{5\text{th percentile} + 95\text{th percentile} - \text{MEDIAN}}{\text{DEVIATION}}$

KURTOSIS =  $\frac{95\text{th percentile} - 5\text{th percentile}}{\text{DEVIATION}^2}$

SAND, SILT, CLAY RELATIONSHIPS - The weight percentages of the total sample falling in the sand (.062 mm or  $4\phi$ ), the silt (.005 mm or  $8\phi$ ), and the clay sizes (.0005 mm or  $11\phi$ ).

SAND/MUD - is a ratio of per cent weight of sand divided by the per cent weight of smaller-than-sand.

PHI SIZE - as elsewhere in this thesis, the phi notation refers to the size of the particle according to the convention:  $-\text{Log}_2$  (size in mm) =  $\phi$ .

Inman Values are used exclusively throughout this paper.

UNCLASSIFIED TECHNICAL REPORTS DISTRIBUTION LIST  
for OCEANOGRAPHIC CONTRACTORS  
of the GEOPHYSICS BRANCH  
of the OFFICE OF NAVAL RESEARCH  
(Revised August 1964)

DEPARTMENT OF DEFENSE

- |   |   |
|---|---|
| 1 Director of Defense Research<br>& Engineering<br>Attn: Coordinating Committee<br>on Science<br>Pentagon<br>Washington, D.C. | 1 Commanding Officer<br>Office of Naval Research Branch<br>1000 Geary Street<br>San Francisco, California 94109 |
| 1 Attn: Office, Asst. Director<br>(Research)  | 1 Commanding Officer<br>Office of Naval Research Branch<br>1030 East Green Street<br>Pasadena, California 91101 |

Navy

- |   |  |
|---|--|
| 2 Office of Naval Research<br>Geophysics Branch (Code 416)<br>Washington, D.C. 20360                            | 10 Commanding Officer<br>Office of Naval Research Branch<br>Navy #100, Fleet Post Office<br>New York, New York                       |
| Office of Naval Research<br>Washington, D.C. 20360  | 1 Oceanographer<br>Office of Naval Research<br>Navy #100, Box 39<br>Fleet Post Office<br>New York, New York                          |
| 1 Attn: Biology Branch (Code 446)   | 1 Contract Administrator<br>Southeastern Area<br>Office of Naval Research<br>2110 "G" Street, N.W.<br>Washington, D.C. 20007         |
| 1 Attn: Surface Branch (Code 463)   | 1 ONR Special Representative<br>c/o Hudson Laboratories<br>Columbia University<br>145 Palisade Street<br>Dobbs Ferry, New York 10522 |
| 1 Attn: Undersea Programs (Code 466)  | 1 Your Resident Representative<br>Office of Naval Research   |
| 1 Attn: Field Projects (Code 418)   |  |
| 1 Commanding Officer<br>Office of Naval Research Branch<br>495 Summer Street<br>Boston, Massachusetts 02110     |  |
| 1 Commanding Officer<br>Office of Naval Research Branch<br>207 West 24th Street<br>New York, New York 10011     |  |
| 1 Commanding Officer<br>Office of Naval Research Branch<br>230 North Michigan Avenue<br>Chicago, Illinois 60601 |  |

- 6 Director  
 Naval Research Laboratory  
 Attn: Code 5500  
 Washington, D.C.
- (Note: 3 copies are forwarded by the above addressee to the British Joint Services Staff for further distribution in England and Canada.)
- 1 Oceanographer  
 Office of the Chief of Naval Operations  
 OP-09B5  
 Washington, D.C.
- 1 Commander  
 U.S. Naval Oceanographic Office  
 Washington, D.C.  
 Attn: Library (Code 1640)
- 1 U.S. Naval Branch  
 Oceanographic Office  
 Navy 3923, Box 77, FPO  
 San Francisco, California
- Chief, Bureau of Naval Weapons  
 Department of the Navy  
 Washington, D.C.
- 1 Attn: FASS  
 1 Attn: RU-222
- 1 Office of the U.S. Naval  
 Weather Service  
 U.S. Naval Station  
 Washington, D.C.
- 1 Chief, Bureau of Yards & Docks  
 Office of Research  
 Department of the Navy  
 Washington, D.C.  
 Attn: Code 70
- 1 Commanding Officer & Director  
 U.S. Navy Electronics Laboratory  
 San Diego, California 92152  
 1 Attn: Code 3102  
 1 Attn: Code 3060C

- 1 Commanding Officer & Director  
 U.S. Naval Civil Engineering  
 Laboratory  
 Port Hueneme, California  
 Attn: Code L54
- Commanding Officer  
 Pacific Missile Range  
 Pt. Mugu, California
- 1 Attn: Code 3145  
 1 Attn: Code 3250
- 1 Commander, Naval Ordnance Lab.  
 White Oak, Silver Spring, Md.  
 Attn: E. Liberman, Librarian
- Commanding Officer  
 Naval Ordnance Test Station  
 China Lake, California
- 1 Attn: Code 753  
 1 Attn: Code 502
- 1 Commanding Officer  
 Naval Radiological Defense Lab.  
 San Francisco, California
- 1 Commanding Officer  
 U.S. Naval Underwater  
 Ordnance Station  
 Newport, Rhode Island
- Chief, Bureau of Ships  
 Department of the Navy  
 Washington, D.C.
- 1 Attn: Code 373
- 1 Officer-in-Charge  
 U.S. Navy Weather Research  
 Facility  
 Naval Air Station, Bldg. R-48  
 Norfolk, Virginia
- 1 U.S. Fleet Weather Facility  
 U.S. Naval Station  
 San Diego, California
- 1 Commanding Officer  
 U.S. Navy Air Development Center  
 Johnsville, Pennsylvania  
 Attn: NADC Library

- 1 Superintendent  
U.S. Naval Academy  
Annapolis, Maryland
- 2 Department of Meteorology &  
Oceanography  
U.S. Naval Postgraduate School  
Monterey, California
- 1 Commanding Officer  
U.S. Naval Underwater Sound Lab.  
New London, Connecticut
- 1 Commanding Officer  
U.S. Navy Mine Defense Laboratory  
Panama City, Florida
- 1 Commanding Officer  
U.S. Fleet Weather Central  
Department of the Navy  
Washington, D.C.
- 2 Officer-in-Charge  
U.S. Fleet Numerical Weather  
Facility  
U.S. Naval Postgraduate School  
Monterey, California

#### Air Force

- 1 Hdqtrs., Air Weather Service  
(AWSS/TIPD)  
U.S. Air Force  
Scott Air Force Base, Illinois
- 1 ARCRL (CRZF)  
L. G. Hanscom Field  
Bedford, Massachusetts

#### Army

- 1 Army Research Office  
Office of the Chief of R & D  
Department of the Army  
Washington, D.C.
- 1 U.S. Army Beach Erosion Board  
5201 Little Falls Road; N.W.  
Washington, D.C.
- 1 Army Research Office  
Washington, D.C.  
Attn: Environmental Sciences Div.

#### OTHER U.S. GOVERNMENT AGENCIES

- 1 Office of Technical Services  
Department of Commerce  
Washington, D.C.
- 20 Defense Documentation Center  
Cameron Station  
Alexandria, Virginia
- 2 National Research Council  
2101 Constitution Avenue, N.W.  
Washington, D.C.  
Attn: Committee on Undersea  
Warfare  
Attn: Committee on Oceanography
- 1 Laboratory Director  
Biological Laboratory  
Bureau of Commercial Fisheries  
P.O. Box 6121, Pt. Loma Street  
San Diego, California
- 1 Commandant (OSR-2)  
U.S. Coast Guard  
Washington, D.C.
- 1 Commanding Officer  
Coast Guard Oceanographic Unit  
Bldg. 159-E, Navy Yard Annex  
Washington, D.C. 20390
- 1 Director  
Coast & Geodetic Survey  
U.S. Department of Commerce  
Washington, D.C.  
Attn: Office of Oceanography
- 1 Geological Division  
Marine Geology Unit  
U.S. Geological Survey  
Washington, D.C.
- 1 Director of Meteorological Research  
U.S. Weather Bureau  
Washington, D.C.
- 1 Director  
U.S. Army Engineers Waterways  
Experiment Station  
Vicksburg, Mississippi  
Attn: Research Center Library

- 1 Laboratory Director  
Bureau of Commercial Fisheries  
Biological Laboratory  
450-B Jordan Hall  
Stanford, California
- 1 Bureau of Commercial Fisheries  
U.S. Fish & Wildlife Service  
Post Office Box 3830  
Honolulu 12, Hawaii
- 1 Attn: Librarian
  
- 1 Laboratory Director  
Biological Laboratory  
Bureau of Commercial Fisheries  
P.O. Box 3098, Fort Crockett  
Galveston, Texas
- 1 Laboratory Director  
Biological Laboratory, Auke Bay  
Bureau of Commercial Fisheries  
P.O. Box 1155  
Juneau, Alaska
- 1 Laboratory Director  
Biological Laboratory  
Bureau of Commercial Fisheries  
P. O. Box 6  
Woods Hole, Massachusetts
- 1 Laboratory Director  
Biological Laboratory  
Bureau of Commercial Fisheries  
P.O. Box 280  
Brunswick, Georgia
- 1 Laboratory Director  
Biological Laboratory  
Bureau of Commercial Fisheries  
P.O. Box 271  
La Jolla, California
  
- 1 Bureau of Sport Fisheries &  
Wildlife  
U.S. Fish and Wildlife Service  
Sandy Hook Marine Laboratory  
P.O. Box 428  
Highlands, New Jersey  
Attn: Librarian

- 1 Director  
National Oceanographic Data Center  
Washington, D.C.
- 2 Defence Research Member  
Canadian Joint Staff  
2450 Massachusetts Avenue, N.W.  
Washington, D.C.
- 2 Library, U.S. Weather Bureau  
Washington, D.C.
  
- 1 Director, Biological Laboratory  
Bureau of Commercial Fisheries  
Navy Yard Annex, Building 74  
Washington, D.C.
- 1 Director, Bureau of Commercial  
Fisheries  
U.S. Fish & Wildlife Service  
Department of Interior  
Washington, D.C.
  
- 1 Dr. Orlo E. Childs  
U.S. Geological Survey  
345 Middlefield Road  
Menlo Park, California
- 1 Dr. John S. Schlee  
U.S. Geological Survey  
c/o Woods Hole Oceanographic  
Institution  
Woods Hole, Massachusetts
  
- 1 Chief of Scientific & Technical  
Publication Staff  
Office of Director  
U.S. Coast & Geodetic Survey  
Mailing Code C-12  
Washington, D.C.

#### RESEARCH LABORATORIES

- 2 Director  
Woods Hole Oceanographic  
Institution  
Woods Hole, Massachusetts

- 3 Project Officer  
Laboratory of Oceanography  
Woods Hole, Massachusetts
- 1 Director  
Narragansett Marine Laboratory  
University of Rhode Island  
Kingston, Rhode Island
- 1 Bingham Oceanographic Laboratories  
Yale University  
New Haven, Connecticut
- 1 Gulf Coast Research Laboratory  
Ocean Springs, Mississippi  
Attn: Librarian
- 1 Chairman, Department of Meteorology  
and Oceanography  
New York University  
New York, New York
- 1 Director  
Lamont Geological Observatory  
Columbia University  
Palisades, New York
- 1 Director  
Hudson Laboratories  
145 Palisade Street  
Dobbs Ferry, New York
- 1 Great Lakes Research Division  
Institute of Science & Technology  
University of Michigan  
Ann Arbor, Michigan
- 1 Attn: Dr. John C. Ayers
- 1 Dr. Harold Haskins  
Rutgers University  
New Brunswick, New Jersey
- 1 Director  
Chesapeake Bay Institute  
John Hopkins University  
Baltimore, Maryland
- 1 Mail No. 353  
The Martin Company  
Baltimore 3, Maryland  
Attn: J. D. Pierson
- 1 Mr. Henry D. Simmons, Chief  
Estuaries Section  
Waterways Experiment Station  
Corps of Engineers  
Vicksburg, Mississippi
- 1 Director, Marine Laboratory  
University of Miami  
#1 Rickenbacker Causeway  
Miami, Florida 33149
- 1 Nestor C. L. Granelli  
Department of Geology  
Columbia University  
Palisades, New York
- 2 Head, Department of Oceanography  
& Meteorology  
Texas A & M University  
College Station, Texas
- 1 Director  
Scripps Institution of Ocean-  
ography  
La Jolla, California
- 1 Allan Hancock Foundation  
University Park  
Los Angeles 7, California
- 1 Head, Department of Oceanography  
Oregon State University  
Corvallis, Oregon
- 1 Department of Engineering  
University of California  
Berkeley, California
- 1 Director  
Arctic Research Laboratory  
Barrow, Alaska

- 1 Dr. C. I. Beard  
Boeing Scientific Research Lab.  
P.O. Box 3981  
Seattle, Washington
- 1 Head, Department of Oceanography  
University of Washington  
Seattle, Washington
- 1 Geophysical Institute of the  
University of Alaska  
College, Alaska
- 1 Director  
Bermuda Biological Station  
for Research  
St. Georges, Bermuda
- 1 Technical Information Center,  
CU-201  
Lockheed Missile & Space Division  
3251 Hanover Street  
Palo Alto, California
- 1 University of Pittsburgh  
Environmental Sanitation  
Department of Public Health  
Practice  
Graduate School of Public Health  
Pittsburgh, Pennsylvania
- 1 Director  
Hawaiian Marine Laboratory  
University of Hawaii  
Honolulu, Hawaii
- 1 Dr. F. B. Berger  
General Precision Laboratory  
Pleasantville, New York
- 1 Dr. J. A. Gast  
Wildlife Building  
Humboldt State College  
Arcata, California
- 1 Department of Geodesy & Geophysics  
Cambridge University  
Cambridge, England
- 1 Applied Physics Laboratory  
University of Washington  
1013 NE Fortieth Street  
Seattle, Washington
- 1 Documents Division - ml  
University of Illinois Library  
Urbana, Illinois
- 1 Director  
Ocean Research Institute  
University of Tokyo  
Tokyo, Japan
- 1 Marine Biological Association  
of the United Kingdom  
The Laboratory  
Citadel Hill  
Plymouth, England
- 1 Central Library  
Lockheed-California Company  
Dept. 72-25, Bldg. 63-1, Plant  
A-1  
Burbank, California
- 1 New Zealand Oceanographic  
Institute  
Department of Scientific &  
Industrial Research  
P.O. Box 8009  
Wellington, New Zealand  
Attn: Librarian
- 1 President  
Osservatorio Geofisico Speri-  
mentale  
Trieste, Italy
- 1 Advanced Research Projects  
Agency  
Attn: Nuclear Test Detection  
Office  
The Pentagon  
Washington, D.C.
- 1 Director  
Water Chemistry Department  
Hydraulic Laboratory  
University of Wisconsin  
Madison, Wisconsin 53706

American Biophysical Research Lab.  
P.O. Box 552  
Lansdale, Pennsylvania

Department of Geology & Geophysics  
Massachusetts Institute of Technology  
Cambridge, Massachusetts

Institute of Geophysics  
University of Hawaii  
Honolulu, Hawaii

Dr. Wilbur Marks  
Oceanics, Inc.  
Technical Industrial Park  
Plainview, New York

Mr. Neil L. Brown  
Bissett-Berman Corporation  
2941 Nebraska Avenue  
Santa Monica, California

Dr. Keith E. Chave  
Marine Science Center  
Lehigh University  
Bethlehem, Pennsylvania